SUBDUCTION SIGNATURE OF THE VARDAR OPHIOLITE OF NORTH MACEDONIA: NEW CONSTRAINTS FROM GEOCHEMICAL AND STABLE ISOTOPE DATA

Valentina Brombin*,, Edoardo Barbero*,***,✉, Emilio Saccani*, Nicola Precisvalle*, Sonja Lepitkova°, Ivica Milevski°°, Igor Ristovski°°°, Igor Milcov°°°, Gorgi Dimov•** and **Gianluca Bianchini*,****

* *Department of Physics and Earth Sciences, University of Ferrara, Ferrara, Italy.*
** *Institute of Environmental Geology and Geoengineering of the Italian National Research Council (CNR-IGAG), Montelibretti, Italy.*
*** *Institute of Geoscience and Earth Resources of the National Research Council (IGG-CNR), Turin, Italy.*
° *Department for Petrology, Mineralogy and Geochemistry, Goce Delcev University of Štip, Republic of Macedonia.*
°° *Department of Geography, Faculty of Natural Sciences and Mathematics, Ss. Cyril and Methodius University in Skopje, Republic of Macedonia.*
°°° *GAYA-CER Non-Governmental Organization, Skopje, Republic of Macedonia.*
• *Faculty of Natural and Technical Sciences, Goce Delčev University, Štip, Republic of Macedonia.*
✉ *Corresponding author, email: brbdrd@unife.it*

Keywords: *Vardar ophiolites; geochemistry; carbon and sulphur isotopes; Jurassic; Demir Kapija; North Macedonia.*

ABSTRACT

Volatiles such as carbon (C) and sulphur (S) are commonly transferred into the mantle from subduction of oceanic lithosphere and overlying sediments. C and S isotopic signatures of magmatic rocks could be used as proxies of the slab components involved in the petrogenesis of subduction-related ophiolites. Therefore, in this work we investigated the major and trace element composition, as well as the C and S elemental contents and isotopic ratios ($^{13}C/^{12}C$ and $^{34}S/^{32}S$) of subvolcanic and volcanic rocks of the Vardar ophiolites of North Macedonia, which represent the remnants of the Mesozoic Tethyan oceanic lithosphere formed in supra-subduction zone tectonic settings.

The ophiolites were sampled at Lipkovo and Demir Kapija localities, in the northern and southern part of North Macedonia, respectively. Based on whole-rock major and trace element composition, three groups of rocks can be distinguished: i) Group 1 rocks, which are subalkaline basalts having backarc affinity, ii) Group 2a and iii) Group 2b rocks, which are calc-alkaline basalts having arc affinity, with and without adakitic signatures, respectively. The qualitative petrogenetic models indicate that studied rocks formed by partial melting of mantle sources variably metasomatized by subduction-related components, such as aqueous fluids, sediment melts, and adakitic melts. Accordingly, all the North Macedonia ophiolites are characterized by C and S signatures which deviate from those typical for mantle and Mid Ocean Ridge melts. The variably low $\delta^{13}C$ values recorded by Group 1 and 2 rocks could be related to the different contributions of melts released by subducting sediments rich in organic matter. However, we cannot exclude that such C-enriched signature is the result of isotopic fractionation during degassing process. In contrast, the enriched S isotopic signatures of the North Macedonia ophiolites suggest a major involvement of melts derived from the subducting sediments rich in sulphate phases. In particular, the calc-alkaline basalts of Group 2 rocks record more positive $\delta^{34}S$ values than the subalkaline basalts of Group 1 formed in backarc basin suggesting that the subarc mantle sources were more affected by slab-released fluids than those of the backarc basin, which were more distal from the trench.

INTRODUCTION

Subduction of oceanic lithosphere plays a crucial role in the cycle of Earth's volatiles (*e.g.*, H, C, S, B, and Cl; Wallace, 2005; Zellmer et al., 2015; Bekaert et al., 2021). In subduction zones, volatiles are transferred from the subducting slab to the overlying subarc mantle wedge by fluids and melts released from the downgoing slab by pore-water release, dehydration processes or melting (Wallace, 2005; Li et al., 2021). This volatile flux plays a fundamental role for the metasomatism of the subarc mantle, which, in turn, controls the composition of volcanic arc rocks (de Hoog et al., 2001; Zellmer et al., 2015; Black and Gibson, 2019). Among the volatiles, carbon (C) and sulphur (S) are transferred into the mantle from subduction of sediments and basaltic crust (Bénard et al., 2018; Schwarzenbach et al., 2018; Walters et al., 2019). According to these authors, C and S of subducting sediments and oceanic crust have isotopic signatures distinguishable from those of typical mantle, and thus may be used as proxies of the nature of the slab components. However, sources, fluxes, and effects of C and S input in the subduction zone are still poorly constrained. Few C and S isotopic studies were focused on melt inclusions, which potentially preserve the original budget and isotopic signature of the magma (Gurenko et al., 2005; Ruth et al., 2018), but these studies are limited, as melt inclusions are not common. Studying volcanic arc and subduction-related rocks exposed within accretionary and collisional belts may therefore represent a valid alternative to investigate contents and isotopic features of volatiles with the aim to reconstruct their cycle during subduction processes. Ophiolites are fragments of ancient oceanic lithosphere that were tectonically emplaced into orogenic belts. On the basis of structural architecture and geochemical features of the magmatic rocks, ophiolites were classified as subduction-unrelated and subduction-related (Dilek, 2003; Dilek and Furnes, 2011; 2014; Saccani, 2015; Furnes et al., 2020). In particular, the latter are thought to be formed in the extending upper plate of ancient subduction zones and their evolution is governed by slab dehydration, melting of the subducting sediments, metasomatism of the subarc mantle, and repeated events of partial melting of metasomatized mantle (Dilek and Furnes, 2011). Hence, the investigation

of volatile elements hosted in subduction-related ophiolites may provide fundamental information to infer the petrogenetic processes and the volatile flux in the mantle wedge. The aim of this paper is to investigate the sources of the volatiles and their different contributions during the petrogenesis of the subvolcanic and volcanic rocks of the Vardar ophiolites of North Macedonia (Fig. 1a), which represent the remnants of the Mesozoic Tethyan oceanic lithosphere formed in a supra-subduction zone (SSZ) tectonic setting (Božović et al., 2013). To this purpose, we performed whole-rock chemical analyses of lithophile elements and mineral chemistry analyses to constrain the geochemical affinity and the petrogenesis of these ophiolitic rocks. In addition, we characterized for the first time their C and S elemental and isotopic ($^{13}C/^{12}C$ and $^{34}S/^{32}S$) composition to constrain the sources of the volatiles and their different contributions during the petrogenesis of the primary magmas. However, other processes occurring in the crustal surface can mobilize C and S and modify the original isotopic signature of the rocks, such as degassing of melts and alteration of rocks in submarine and subaerial environments. Therefore, we firstly demonstrated that C and S isotope signatures are inherited by processes occurring in the mantle, i.e., before the eruptions of melts, rather than by processes of alteration of the rocks. This work may shed light on the complexity and heterogeneity of the sources and processes responsible for the volatiles in the subduction zone and testify that subduction-related ophiolites are potential archives of the volatile flux and fluids/melts release within subduction zones.

GEOLOGICAL SETTING

Geological setting of the Dinaric-Hellenic belt

The North Macedonia is part of the Dinaric-Hellenic belt (Fig. 1a), which is an Alpine collisional belt extending from Slovenia to southern Greece. The Dinaric-Hellenic belt resulted from the Mesozoic-Cenozoic convergence between the Adria microplate and the Eurasia plate that was accommodated by the closure of the Tethyan Ocean, ophiolite obduction, and continental collision (Robertson and Shallo, 2000; Pamić et al., 2002; Karamata, 2006; Dilek et al., 2007; Schmid et al., 2008; Robertson et al., 2009; Bortolotti et al., 2013; Boev et al., 2018; Maffione and van Hinsenbergen, 2018). In the southern part of the Dinaric-Hellenic belt (i.e., from Albania-North Macedonia to Greece), five west-verging main tectono-stratigraphic zones have been identified, from west to east: i) the Deformed Adria zone; ii) the Dinaric-Mirdita-Pindos ophiolitic zone (Subpelagonian zone); iii) the Korabi-Pel-

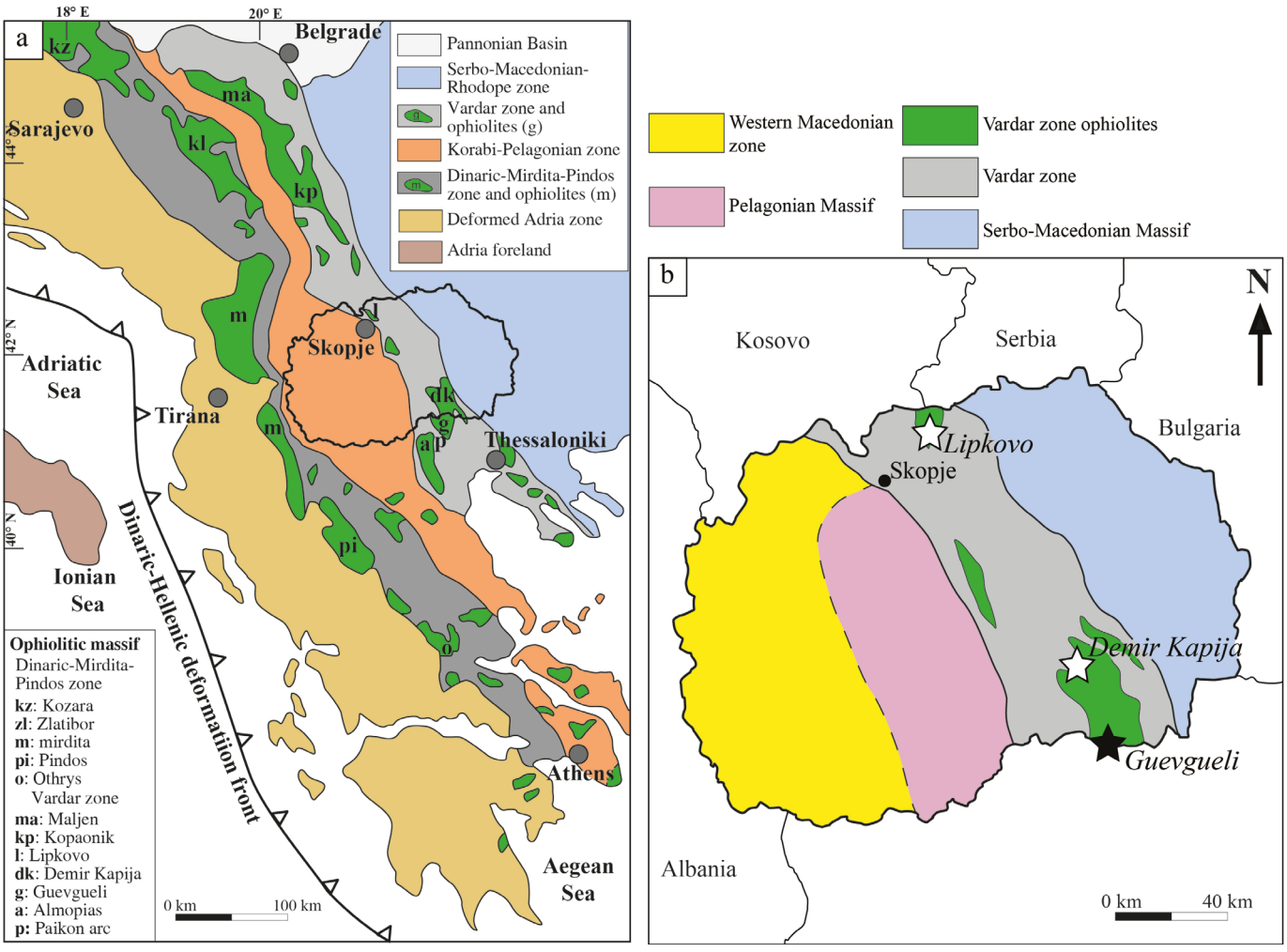

Fig. 1 - a) Simplified tectonic map of the Dinaric-Hellenic belt showing the main zones and ophiolites (modified from Saccani et al., 2011). b) Geological map of the North Macedonia with the main geological units (modified from Šoster et al., 2020, Petrušev et al., 2021). The white stars indicate the sampling locations of this study. The location of the Guevgeli Complex (black star) is also reported.

agonian zone; iv) the Vardar ophiolitic zone; v) the Serbo-Macedonian-Rhodope zone (Fig. 1a; Robertson and Shallo, 2000; Chiari et al., 2011; Ferrière et al., 2012; Bortolotti et al., 2013). The Deformed Adria zone is composed of several tectonic units showing Triassic to Miocene sedimentary succession representing the original sedimentary cover of the Adria microplate (Robertson and Shallo, 2000; Dilek et al., 2007). The Mirdita-Pindos ophiolitic zone is characterized by several Triassic-Jurassic ophiolites and related sedimentary successions (Bébien et al., 2000; Saccani et al., 2011; 2017). These ophiolites show magmatic rocks with geochemical affinity ranging from mid-ocean ridge basalt (MORB) to island arc tholeiites (IAT), and boninites (Beccaluva et al., 1994; Dilek et al., 2007; Saccani et al., 2011). These ophiolites are interpreted as generated in a SSZ setting and record the evolution from nascent forearc to mature intra-oceanic arc. The Korabi-Pelagonian zone is made up by an assemblage of tectonic units, which includes rocks derived from a Paleozoic metamorphic basement and the overlain Permo-Triassic to Jurassic sedimentary cover (Robertson and Shallo, 2000; Tremblay et al., 2015). In the North Macedonia, the Korabi-Pelagonian zone is subdivided into two distinct zones, which are the West-Macedonian zone and the Pelagonian Massif (Fig. 1b). The West-Macedonian zone is composed of low-grade metamorphic and magmatic Paleozoic rocks, Triassic and Jurassic sedimentary and magmatic rocks, as well as Cenozoic sedimentary successions. The Pelagonian Massif is a relic of a dome-shaped Proterozoic crystalline basement. The boundary with the West-Macedonian zone is represented by a deep regional reverse fault (see Petrušev et al., 2021, and references therein). The geodynamic interpretation of the Korabi-Pelagonian zone is rather controversial. In fact, it has been interpreted either as a continental domain separating two oceanic basins, the Mirdita-Pindos and Vardar ocean (e.g., Robertson, 2002; Karamata, 2006; Dilek et al 2007; Robertson et al., 2009) or as the distal part of the Adria Microplate margin structurally exposed as a tectonic window below a far-travelled ophiolitic nappe derived from a single Mesozoic oceanic basin (e.g., Saccani et al., 2008b; Schmid et al., 2008; Kilias et al., 2010; Saccani et al., 2011; Ferrière et al., 2012; Bortolotti et al., 2013; Tremblay et al., 2015). The Vardar zone consists of a composite structural assemblage made up of both continental- and oceanic-derived units (Robertson et al., 2009). The studied ophiolites are included within this zone that, therefore, will be described in detail in the following section. Finally, the Serbo-Macedonian-Rhodope zone is composed of high to medium grade meta-igneous and metasedimentary rocks and it is interpreted as the westernmost European margin during Mesozoic convergence (Šarić et al., 2009; Božović et al., 2013).

Vardar zone

The Vardar zone represents a NNW-SSE striking elements interposed between the Korabi-Pelagonian and the Serbo-Macedonian-Rhodope zones (Fig. 1a). This zone shows Triassic-Jurassic and largely dismembered ophiolites that are also known as Inner Hellenic ophiolites (Smith, 1993). Different sub-zones have been distinguished and named by several authors working in different segments of the Dinaric-Hellenic belts (e.g., Mercier, 1966; Pe-Piper and Piper, 2002; Schmid et al. 2008). In the Macedonian Greece, from west to east the Vardar zone is subdivided into the Almopias, Paikon, and Peonias (i.e., Guevgueli) sub-zones (Mercier, 1966; Pe-Piper and Piper, 2002; Saccani et al., 2015). In the northern part of the belt (i.e., in the central and northern Serbia area), the Vardar zone is subdivided into the Western Vardar zone and the Main Vardar zone, which are separated by the Kopaonik unit (Robertson et al., 2009). Regardless of the different nomenclature, these different sub-zones can basically be correlated each other. Here we follow the sub-zones described for the Northern Greece sector, because the Demir-Kapija ophiolites studied in this paper continues in northern Greece, where they are known as Guevgueli ophiolites.

The Almopias sub-zone is tectonically rather complex and is mainly composed of Jurassic ophiolites and related sedimentary cover (Sharp and Robertson, 1994; Saccani et al., 2008b; 2015). In this sub-zone, the ophiolites are highly dismembered and mantle rocks tectonically overlay a sub-ophiolitic mélange including ophiolitic rocks showing MORB, IAT, and boninitic affinities (Saccani et al., 2008b; 2015). These ophiolites are interpreted as SSZ ophiolites formed in an intra-oceanic island arc setting (Saccani et al., 2008b; 2011).

The Paikon sub-zone includes Triassic to Late Jurassic metamorphic successions composed of metasedimentary and metavolcanic rocks (Mercier, 1966; Sharp and Robertson, 1994). The latter show geochemical features suggesting a volcanic arc affinity. These assemblages are interpreted as representing a Middle to Late Jurassic volcanic arc (Paikon arc) formed onto the continental margin of Eurasia plates because of an east-dipping subduction (Mercier, 1966; Vergély and Mercier, 2000).

Finally, the Guevgueli sub-zone includes two ophiolites, namely Guevgueli (in northern Greece) and Demir Kapija (in North Macedonia). The Late Jurassic Guevgueli ophiolites composed of gabbros, dykes, and lavas showing backarc basin basalt (BABB) as well as calc-alkaline (CAB) chemical affinities (Bébien et al., 1986; Saccani et al., 2008a). The lavas are associated with radiolarian cherts indicating a Late Jurassic age (Saccani et al., 2011 and reference therein). The ophiolite is intruded by Late Jurassic granites associated with migmatites and magmatic breccias (Bébien et al., 1986; Šarić et al., 2009). Collectively, this assemblage is interpreted as formed in a Late Jurassic backarc basin that was existing between the Paikon arc and the Eurasian margin (*i.e.*, the Serbo-Macedonian-Rhodope zone). The Demir Kapija ophiolite represents, in fact, the continuation of the Guevgueli sub-zone in North Macedonia (Božović et al., 2013). It is composed of gabbros, diabases, and pillow lavas associated with intermediate and acid magmatic intrusions having subduction-related affinity (Šarić et al., 2009) and locally bearing an adakitic signature (Demir Kapija; Božović et al., 2013; Boev et al., 2018). In the ophiolites from the Guevgueli sub-zone, peridotites are very rare (Šarić et al., 2009; Boev et al., 2018). The age of the BABB and MORB crust of the southern Vardar ophiolites is ~ 166 Ma, according to radiolarian biostratigraphic dating of cherts associated with volcanic rocks within the Guevgueli complex (Kukoč et al., 2015) and U/Pb datings of Demir Kapija gabbros (Božović et al., 2013). The subduction-related rocks of Demir Kapija record an age of ~ 164 Ma, indicating they are temporally close to the formation of the BABB and MOR oceanic crust (Božović et al., 2013).

SAMPLING AND PETROGRAPHY

For this study seventeen samples of subvolcanic and volcanic rocks were collected from different ophiolitic outcrops

along the central part of the North Macedonia. Twelve samples were collected from the well-known Demir Kapija ophiolite, in the southern North Macedonia which is composed of gabbros, diabases, and pillow lavas with variable geochemical compositions, from MOR- to SSZ-affinity (Šarić et al., 2009; Božović et al., 2013). Other five samples were collected near Lipkovo in the northern part of North Macedonia (Fig. 1b). The Lipkovo ophiolitic complex, also known as Lojane ophiolitic complex (Augé et al., 2017), has been poorly investigated in literature. It is mainly characterized by a basal mantle sequence with harzburgite and minor dunite overlain by the cumulate sequence consisting of basal dunite, followed by lherzolite, pyroxenite and gabbro, and a volcanosedimentary sequence with basaltic pillow lava (Augé et al., 2017). The global positioning system (GPS) coordinates of the sampled points both in Demir Kapjia and Lipkovo are reported in Table 1. The samples are subvolcanic and volcanic rocks having basaltic compositions. The subvolcanic rocks were sampled both in Demir Kapija and Lipkovo, whereas the volcanic rocks are only from Demir Kapija.

Most of the studied rocks are affected by various degrees of low-grade ocean-floor hydrothermal alteration. Olivine is mainly replaced by iddingsite, plagioclase is sometimes pseudomorphosed by albite and sericite. In volcanic rocks, volcanic glass is replaced by chlorite and clay minerals. Only clinopyroxene occurs as fresh crystals, though in some samples it is replaced by amphibole and/or chlorite. In some samples amygdales and veins filled with calcite are also present. Subvolcanic rocks show holocrystalline and inequigranular texture. They are characterized by euhedral plagioclases (up to 4 mm across), smaller subhedral to anhedral clinopyroxenes (up to 2 mm across), and Fe-Ti oxides (up to 1 mm across). The olivine is rare and altered to iddingsite (up to 1 mm across). Volcanic rocks show aphyric (PI <10) and weakly porphyritic (PI = 15-20) textures. In the aphyric rocks the groundmass is hypocrystalline with microlites of plagioclase and small crystals of olivine, clinopyroxene, and Fe-Ti oxides. In weakly porphyritic basalts, the phenocrysts consist of euhedral to subhedral plagioclase (up to 3-4 mm across), subhedral clinopyroxene (up to 1 mm across), and minor olivine (up to 1-2 mm across). The phenocrysts are set in an intersertal groundmass composed by microlites of plagioclase, olivine, clinopyroxene, minor glass, and Fe-Ti oxides.

ANALYTICAL METHODS

X-ray powder diffraction (XRD) analyses were performed on six samples (DS5, DS6, DS7, DS8, DS13, DS15) to identify the main phases and the alteration products of the ophiolitic rocks, and, therefore, plan the electron probe analyses of the main mineral phases. These samples have been selected as we recognized from petrographic analyses several clinopyroxene and plagioclase rather fresh for electron microprobe analyses. Data collection was performed on Bruker D8 Advance Da Vinci diffractometer working in Bragg-Brentano geometry equipped with a LynxEye XE silicon strip detector (angular range of the detector window size = 2.585° 2θ) set to discriminate Cu Kα1,2 radiation, Ni-filter to suppress Cu Kβ component. The powder was placed within a sample holder and scanned in a continuous mode from 5 to 80° 2θ with step size of 0.02° 2θ and a counting time of 1 s per step. Qualitative phase analysis of collected patterns was performed by means of the Bruker AXS EVA software (v.5).

The major element composition of the main phases (plagioclase and clinopyroxene), as well as oxides were obtained by electron microprobe (EMP) spectrometry using a CAMECA SX 50 at the Institute of Environmental Geology and Geoengineering (IGAG-CNR) of the University of Rome "La Sapienza" (Italy). Analytical conditions were as follows: 15 kV acceleration potential; beam size focused at 5 μm;15 nA beam current; 20-30 seconds counting time, as a function of the analyzed element. Silicate minerals and synthetic oxides were employed as standards.

Whole rock major and some trace (Zn, Cu, Ni, Co, Cr, V, Ba) elements were analyzed by X-Ray Fluorescence Spectrometry (XRF) at the Department of Chemical and Geological Sciences of Modena and Reggio Emilia University (Italy) using the wavelength dispersive X-Ray fluorescence (Philips PW1480) on pressed pellets and applying the methods of Franzini et al. (1975) and Leoni and Saitta (1976). Analyses are considered accurate within 2-5% for major elements, and better than 10% for trace elements. Volatile contents were determined as loss on ignition (LOI) at 1000°C. The rare earth elements (REE) and some trace elements (Rb, Sr, Zr, Y, Nb, Hf, Ta, Th, U) were determined by Inductively Coupled Plasma-Mass Spectrometry (ICP-MS) using a Thermo Series X-I spectrometer at the Department of Physics and Earth Sciences of the Ferrara University (Italy). The accuracy of the data for XRF and ICP-MS analyses were evaluated using results for international standard rocks run as unknowns. The detection limits for XRF and ICP-MS analyses were evaluated using results from several runs of 29 international standards and are given in the Table 1S.

The analyses of C and S contents (expressed in wt%) and the relative isotope ratios ($^{13}C/^{12}C$, $^{34}S/^{32}S$) were carried out at the Department of Physics and Earth Science of University of Ferrara using an elemental analyser (EA) PYRO Cube (Elementar) operating in combustion mode and coupled with the isotope ratio mass spectrometer (IRMS) precisION (Elementar). Homogenous powdered samples (around 40 mg) were weighed in tin capsules, wrapped, and finally loaded into the elemental analyser. For this analytical system, samples are burnt via flash combustion with O_2 at 1150°C in a quartz "combustion" tube. The gaseous species released by the samples are transferred in a second quartz "reduction" tube (heated at 850°C) and in a water trap to remove the excess of oxygen and water. The formed CO_2, and SO_2 gases are separated by a trap-and-purge module and the relative abundances are quantitatively determined on a thermo-conductivity detector. After the elemental analyses, CO_2, and SO_2 flow in sequence to the coupled IRMS for isotopic composition determination. The calibration of the instruments was performed using several standards: the Carrara Marble (Natali and Bianchini, 2015), the Jacupiranga carbonatite (Beccaluva et al., 2017), the Tibetan human hair powder USGS42 (Coplen and Qi, 2011), and the Barium Sulfate IAEA-SO-5 (Halas and Szaran, 2001). The $^{13}C/^{12}C$ and $^{34}S/^{32}S$ isotopic ratios (R) were expressed with the δ notation (in ‰ units):

$$\delta = (R_{sam}/R_{std} - 1) \times 1000$$

where R_{sam} is the isotopic ratio of the sample and R_{std} is the isotopic ratio of the international isotope standards Pee Dee Belemnite (PDB) and Canyon Diablo troilite (CDT) for C and S, respectively. Analytical uncertainties (1 sigma) for the isotope analyses were in the order of ±0.1‰ for $\delta^{13}C$ and ± 0.3‰ for $\delta^{34}S$, as indicated by repeated analyses of samples and standards.

Table 1 - Major (wt.%) and trace (ppm) composition of subvolcanic and volcanic rocks of North Macedonia ophiolites.

	Tholeiitic affinity			Calc-alkaline affinity													
Locality	Demir Kapija			Demir Kapija									Lipkovo				
Sample	DS13	DS14	DS15	DS7	DS8	DS12	DS3	DS5	DS6	DS9	DS10	DS11	SL1	SL2	SL3	SL4	SL5
Group	Group 1	Group 1	Group 1	Group 2a	Group 2a	Group 2a	Group 2b	Group 2b	Group 2b	Group 2b	Group 2b	Group 2b	Group 2b	Group 2b	Group 2b	Group 2b	Group 2b
Lat (N)	41.18978	41.26469	41.25197	41.33835	41.33836	41.23496	41.42451	41.36849	41.36850	41.32158	41.30118	41.30998	42.19042	42.18451	42.18071	42.17191	42.16486
Long (E)	22.47251	22.65434	22.65111	22.38475	22.38475	22.49617	22.30889	22.34570	22.34570	22.40815	22.41678	22.41357	21.56054	21.56489	21.56858	21.57337	21.57732
XRF																	
SiO_2	54.70	47.90	45.07	46.60	42.29	48.95	41.29	49.42	49.45	51.35	52.00	50.60	49.31	48.15	50.48	50.10	48.86
TiO_2	1.31	1.88	1.30	0.55	0.47	1.24	1.18	0.72	0.74	0.75	1.29	1.11	1.16	2.19	1.51	1.13	1.10
Al_2O_3	12.49	14.24	14.54	14.92	13.71	15.08	12.45	13.09	13.49	13.70	14.99	13.88	15.71	14.46	14.83	15.62	15.82
Fe_2O_3	1.21	1.49	1.47	0.96	0.81	0.99	1.31	0.98	0.96	0.98	1.15	1.17	1.42	1.69	1.15	1.16	1.20
FeO	8.09	9.91	9.80	6.43	5.37	6.61	8.71	6.51	6.40	6.54	7.66	7.80	9.46	11.26	7.70	7.73	8.00
MnO	0.17	0.18	0.19	0.13	0.11	0.14	0.22	0.11	0.12	0.12	0.15	0.15	0.18	0.22	0.17	0.17	0.17
MgO	6.72	7.83	12.02	14.96	14.69	7.51	16.40	10.80	10.70	10.47	7.21	11.77	9.92	7.92	6.52	12.19	10.18
CaO	7.20	8.01	8.51	6.29	11.34	11.14	9.94	7.91	7.61	6.52	6.31	4.92	8.43	5.19	10.38	2.47	7.52
Na_2O	5.02	4.47	3.10	2.02	1.58	3.64	0.54	3.52	3.45	4.96	4.38	3.98	3.05	3.42	3.15	3.36	3.36
K_2O	0.26	0.31	0.13	0.65	0.55	0.81	0.48	1.88	2.14	0.05	0.42	0.60	0.83	0.07	0.21	0.04	0.43
P_2O_5	0.19	0.28	0.14	0.11	0.07	0.26	0.07	0.07	0.07	0.05	0.16	0.15	0.23	0.33	0.34	0.19	0.23
LOI	2.40	3.10	3.46	6.22	8.56	3.47	7.51	4.67	4.41	4.34	3.85	3.39	3.02	4.57	3.49	5.31	2.66
Total	99.76	99.61	99.73	99.84	99.55	99.82	100.09	99.69	99.54	99.83	99.56	99.52	99.72	99.47	99.93	99.46	99.53
Mg#	59.7	58.4	68.6	80.6	83.0	66.9	77.0	74.7	74.9	74.0	62.7	72.9	65.1	55.6	60.1	73.8	69.4
Zn	73	87	86	192	60	66	69	127	168	71	89	76	93	120	88	150	85
Cu	242	67	29	59	65	51	79	56	66	54	50	65	54	43	47	23	18
Ni	13	90	106	146	130	99	392	171	139	142	45	105	96	3	171	49	117
Co	47	61	71	58	61	51	76	59	59	52	58	56	64	47	58	62	57
Cr	42	178	164	209	207	164	357	456	394	325	85	239	198	32	303	90	219
V	377	341	281	217	206	224	186	238	232	194	352	298	257	478	252	290	261
Ba	37	48	34	136	137	237	53	151	129	75	125	161	198	280	147	185	135
ICP-MS																	
Rb	3.99	4.33	2.76	5.66	5.27	15.0	3.94	8.71	11.1	3.66	4.18	5.64	13.6	18.9	6.72	9.50	13.6
Sr	137	210	197	474	330	350	139	170	165	105	200	172	236	250	227	180	162
Y	27.0	38.5	27.0	9.41	13.0	11.7	19.7	21.7	14.5	11.3	30.6	20.6	30.4	43.4	25.7	25.4	29.0
Zr	105	179	126	67.0	65.2	126	90.9	72.0	69.6	59.1	118	90.1	124	210	150	113	125
Nb	3.62	6.39	4.34	1.86	1.79	4.62	1.76	2.83	2.46	2.17	3.70	1.73	2.81	5.61	6.28	3.13	3.36
La	5.34	7.30	5.47	6.96	6.27	15.9	5.46	7.26	5.28	4.77	6.80	5.86	7.95	15.5	16.2	7.49	7.09
Ce	15.4	20.0	14.5	15.3	13.6	30.5	14.1	17.4	12.9	10.9	17.4	15.1	19.8	36.2	34.4	17.8	17.5
Pr	2.46	3.05	2.38	1.78	1.84	3.21	2.09	2.39	1.8	1.46	2.7	2.13	2.84	5.04	4.32	2.7	2.66
Nd	11.7	14.2	11.9	6.58	7.54	10.6	9.71	10.4	7.69	6.55	13.0	9.74	13.3	21.5	17.0	12.4	12.0
Sm	3.59	4.27	3.68	1.71	2.14	2.43	2.98	3.10	2.28	1.85	3.98	2.92	3.91	6.39	4.53	3.37	3.63
Eu	1.23	1.55	1.37	0.53	0.72	0.69	1.03	1.07	0.73	0.62	1.30	0.92	1.17	1.96	1.34	0.99	1.14
Gd	4.43	5.32	4.42	1.72	2.21	2.22	3.32	3.54	2.45	1.98	4.59	3.35	4.45	7.20	4.34	4.02	4.78
Tb	0.78	0.91	0.78	0.28	0.35	0.35	0.57	0.61	0.41	0.33	0.79	0.57	0.76	1.19	0.73	0.68	0.80
Dy	5.01	5.73	4.81	1.78	2.20	2.07	3.63	3.98	2.64	2.10	5.09	3.67	4.84	7.32	4.30	4.31	5.12
Ho	1.07	1.26	1.01	0.37	0.46	0.43	0.76	0.86	0.56	0.44	1.12	0.78	1.05	1.49	0.88	0.92	1.09
Er	2.95	3.38	2.81	0.99	1.30	1.13	2.03	2.37	1.52	1.23	3.11	2.18	2.85	3.98	2.34	2.58	2.96
Tm	0.44	0.50	0.40	0.14	0.19	0.16	0.31	0.36	0.23	0.18	0.46	0.33	0.43	0.57	0.34	0.38	0.43
Yb	2.69	2.96	2.61	0.89	1.18	0.98	1.93	2.22	1.43	1.16	3.00	2.06	2.73	3.56	2.16	2.39	2.66
Lu	0.39	0.41	0.36	0.13	0.17	0.14	0.28	0.33	0.21	0.16	0.44	0.31	0.41	0.51	0.31	0.35	0.39
Hf	3.20	4.46	3.49	1.66	1.91	3.42	2.48	2.55	2.10	1.63	3.53	2.72	3.60	5.07	4.11	3.01	3.59
Ta	0.38	0.51	0.28	0.13	0.14	0.39	0.10	0.33	0.16	0.11	0.21	0.18	0.27	0.47	0.48	0.22	0.25
Th	0.49	0.68	0.37	2.08	2.40	3.77	0.68	1.67	1.19	1.30	1.82	1.45	1.58	3.57	3.10	2.36	1.19
U	0.19	0.27	0.12	0.92	1.07	1.29	0.20	0.40	0.39	0.55	0.62	0.45	0.47	1.32	0.66	0.92	0.36

Mg# = 100 × MgO / (MgO + FeO). Fe2O3 = 0.15 × FeO; LOI: loss on ignition

RESULTS

Phase identification

The XRD patterns are reported in Fig. 1S. In all the investigated rocks the main phases are plagioclase and clinopyroxene. In some samples, other minor phases are also present, such as chlorite (DS6, DS13, DS15), serpentine (DS5, DS7, DS8), and vermiculite (DS7, DS8), as alteration products of olivine and Ca-amphibole (DS13, DS15) as replacement of clinopyroxene. K-feldspar (DS6), and stilbite (DS7, DS8) are rare. In addition, calcite occurs in most of the selected samples (DS5, DS6, DS7, and DS8). A variable amount of oxides are detected as associated phases.

Mineral chemistry

The results of *in-situ* chemical analyses on clinopyroxenes, plagioclases, and oxides are reported in Tables 2S-4S, and classification diagrams are reported in Fig. 1S. The analyses of olivine were not performed, as no fresh crystals were found.

The majority of analyzed clinopyroxene has augitic composition, though some crystals are diopside (Wo_{38-46} En_{41-48} Fs_{7-16}). The clinopyroxene shows a wide range of Mg# values (88-74) and variable TiO_2 (0.29-1.06 wt%), Al_2O_3 (1.56-3.83 wt%), FeO_{tot} (4.32-10.08 wt%), and Na_2O (0.16-0.78 w%) contents. For all the clinopyroxenes, TiO_2, Al_2O_3, and FeO_{tot} contents increase and CaO decrease with the decreasing Mg#. The clinopyroxene composition represents an important petrogenetic indicator of the chemical affinity of the magmatic melts from which they crystallized (Leterrier et al., 1982; Beccaluva et al., 1989). In the discrimination diagram of Beccaluva et al. (1989) the clinopyroxenes plot in the field typical of basalts from SSZ setting (Fig. 2).

Fresh plagioclase crystals are rare. The anorthite content in these crystals is relatively high (73.9%-82.7%) classifying them as labradorite and bytownite. The co-variation of the anorthite content of plagioclase with the Mg# of coexisting clinopyroxene resemble the compositional mineralogy variation of rocks from SSZ ophiolites (Fig. 3).

According to petrographic observation and XRD patterns, the amount of opaque minerals is limited. They are mainly represented by magnetite to Ti-magnetite occurring in the groundmass (MgO 0.09-2.70wt.%; TiO_2 0.61-3.33 wt%).

Whole rock geochemistry

The results are reported in Table 1. The petrographic analyses and the generally high LOI values (2.40-8.56 wt%) indicate that most of the studied rocks have undergone secondary alteration. Large ion lithophile elements (LILE) and many major elements may have been remobilized during these secondary processes (Cann, 1970; Pearce and Norry, 1979). Therefore, for constraining the North Macedonia ophiolites compositions, we preferentially used elements such as Y, V, Ti, Zr, Nb, Ta and REEs which are relatively immobile during low temperature alteration and ocean-floor metamorphism (Pearce and Norry, 1979). In addition, in order to estimate the general amount of remobilization for elements such as Ba, Sr, Rb, and Al_2O_3, mobility tests were performed by plotting them against immobile elements (e.g., Zr, Y) and calculating the correlation coefficient (r^2). The results return r^2 between 0.5-0.75 suggesting that these elements can be used, though with some caution. Based on the geochemical compositions,

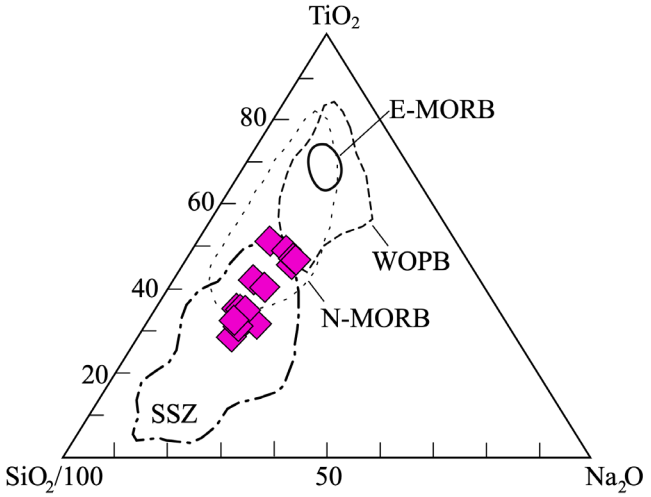

Fig. 2 - TiO_2-Na_2O-SiO_2/100 diagram for discriminating clinopyroxenes in basalts from different oceanic settings (Beccaluva et al., 1989). Abbreviations: E-MORB: enriched mid-ocean ridge basalt; N-MORB: normal midocean ridge basalt; WOPB: within-oceanic plate basalts; and SSZ: supra-subduction zone basalts.

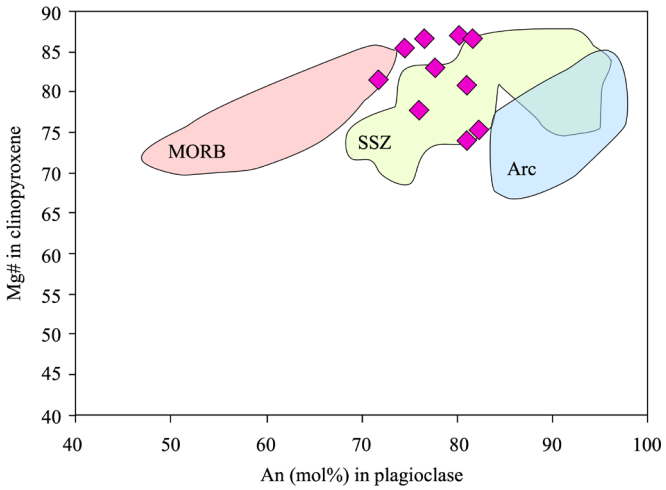

Fig. 3 - Anorthite (An) in plagioclase vs. Mg# in clinopyroxene diagram for subvolcanic and volcanic rocks of North Macedonia ophiolites. Field for compositional variations of supra-subduction zone ophiolites (SSZ), arc gabbros (ARC), and oceanic cumulate (MORB) are shown for comparisons (Burns, 1985; Hébert and Laurent, 1990; Parlak et al., 2020).

the studied subvolcanic and volcanic rocks can be divided into two groups whose geochemistry will be described in the following sections.

Group 1

These rocks were collected in the Demir Kapija area (Fig. 1). They are represented by sub-alkaline basalts, as indicated by low Nb/Y ratio (0.13-0.17; Fig. 4). The SiO_2 (45.1-54.7 wt%), MgO (6.7-12.0 wt%), Mg# (68.6-58.4) and compatible elements (e.g., Cr, Ni, Co, V; Table 1) contents are variable indicating that these rocks derived from melts at different stages of fractionation. These rocks are also characterized by relatively high ranges of TiO_2 (1.3-1.9 wt%) and P_2O_5 (0.14-0.28 wt%).

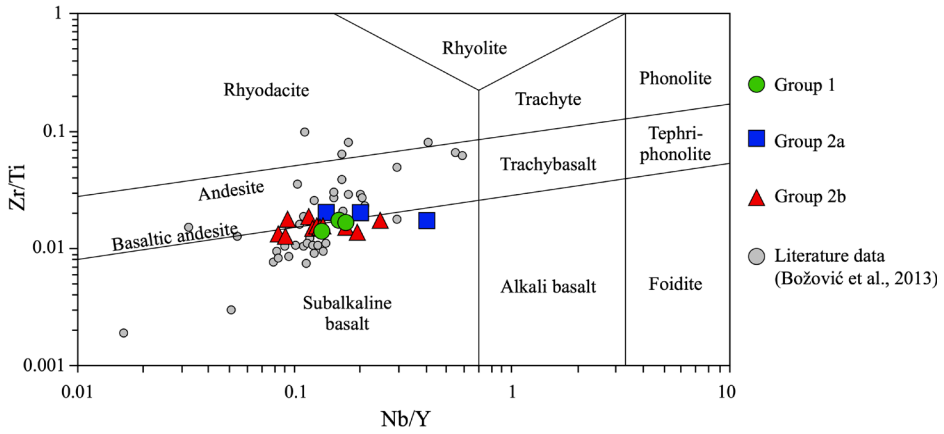

Fig. 4 - Nb/Y vs. Zr/Ti discrimination diagram of Winchester and Floyd (1977) for subvolcanic and volcanic rocks of North Macedonia ophiolites.

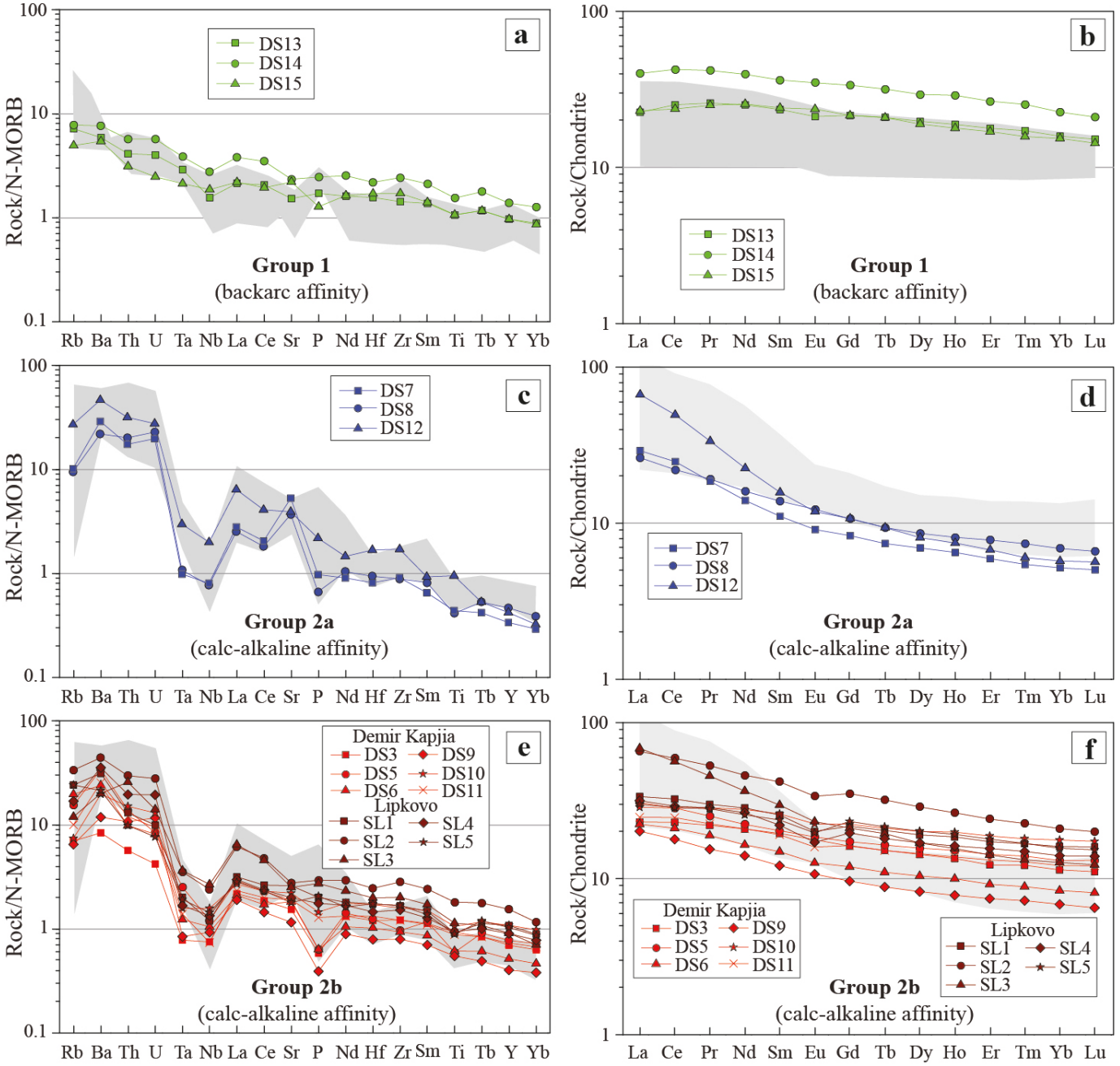

Fig. 5 - N-MORB normalized incompatible element patterns (left column) and chondrite-normalized rare earth element patterns (right column) for subvolcanic and volcanic rocks of North Macedonia ophiolites. N-MORB is chosen as normalizing factor as it is a useful tectonic end-member to outline tectono-magmatic variation of ophiolitic rocks as shown by Pearce (2014). Normalizing values are from Sun and McDonough (1989). The grey field represents the composition of the backarc basin basalts of Guevgueli complex (Saccani et al., 2008b).

In the normal MORB (N-MORB) normalized incompatible element spider-diagrams (Fig. 5a), Group 1 rocks display decreasing patterns from LILEs (e.g., Rb, Ba), U and Th to high field strength elements (HFSEs; e.g., Ta, Nb, Hf, Zr, Sm, Ti, Y, and Yb). The chondrite-normalized REE patterns (Fig. 5b) show a slight enrichment in light (L) REE and no fractionation in heavy (H) REE as testified by the $(La/Yb)_N$ and $(Dy/Yb)_N$ ratios, whose ranges are 1.42-1.77 and 1.23-1.30, respectively. The Group 1 rocks show comparable Ta/Yb (0.11-0.17) and Th/Yb (0.14-0.23) ratios (Fig. 3S), which are close to those typical of E-MORBs (Ta/Yb = 0.20; Ta/Yb = 0.25; Sun and McDonough, 1989). However, the LREE/HREE ratios are higher than MORBs (Fig. 5a, b). These features are consistent with those of BABBs of the Guevgueli ophiolites, which were not influenced or only little affected by subduction materials (Saccani et al., 2008a; Fig. 5a, b). Accordingly, in the discrimination diagrams the rocks of Group 1 plot in the field for BABB (Fig. 6). In particular, in the discrimination diagram of Saccani (2015) the Group 1 rocks fall in the backarc B field (Fig. 6), indicating that they were scarcely affected by chemical components deriving from the subducting slab or crustal assimilation, similar to the BABBs of the Central Dinaric Ophiolite Belt investigated by Lugović et al. (1991), who excluded a contribution of subduction components for their petrogenesis. The North Macedonia ophiolites are probably related to a mature intra-oceanic backarc, as hypothesized for the BABBs of the near Guevgueli complex (Saccani et al., 2008a).

Group 2

These rocks were collected both in the Demir Kapija and Lipkovo areas (Fig. 1a). They include basalts and minor basaltic andesites with sub-alkaline affinity, as Nb/Y values are low and vary over a relatively wide range (0.08-0.24; Fig. 4). In terms of major elements, these rocks exhibit a large variability, showing large variation in SiO_2 (41.3-52.0 wt%), TiO_2 (0.5-2.2 wt%), MgO (6.5-16.4 wt%), Mg# (83.0-55.6), P_2O_5 (0.05-0.35 wt%), and compatible elements (e.g., Cr, Ni, Co, V; Table 1) contents. In the extended incompatible element plots normalized to N-MORB (Fig. 5c, e), the samples of this group are characterized by marked enrichment in LILEs (Rb, Ba), U and Th and depletion in HFSEs (Nb, Ta, and Ti), whereas in the chondrite-normalized REE patterns, the REE display a strong LREE to HREE fractionation [$(La/Yb)_N$ = 1.62 to 11.64; Fig. 5d, f]. Such features are typical of calc-alkaline rocks. In fact, Group 2 rocks show high Th/Yb ratios with respect to Ta/Yb ratios (Fig. 3S), suggesting that these rocks are influenced by an arc geochemical component (Pearce, 1982; Furnes et al., 2020). Accordingly, in the discrimination diagrams these samples plot in the field for SSZ basalts, with composition similar to calc-alkaline basalts (CABs; Fig. 6).

Although Group 2 subvolcanic and volcanic rocks show similar major element and most trace element contents, two different subgroups (Group 2a and 2b) can be identified based on some different trace element contents, REE patterns, and Sr/Y ratios (Fig. 7). Unfortunately, no clear relationships between volcanic and subvolcanic of Groups 2a and 2b can be seen in the field. The subvolcanic and volcanic rocks of Group 2a were collected only in Demir Kapija region, whereas those of Group 2b are both from Demir Kapija and Lipkovo areas. The Group 2a rocks have higher Sr and lower Y contents than Group 2b rocks (Fig. 7; Table 1). In the chondrite-normalized REE patterns, Group 2a rocks show more significant LREE/HREE [$(La/Yb)_N$ = 3.82 to 11.64; Fig. 5d] and MREE/HREE [$(Sm/Yb)_N$ = 2.01 to 2.79; Fig. 5d] enrichments rather than Group 2b [$(La/Yb)_N$ = 1.62 to 5.39; $(Sm/Yb)_N$ = 1.47 to 2.33; Fig. 5e]. In general, the high LREE/HREE coupled with the high Sr/Y ratios of all subvolcanic and volcanic of Group 2a point to an adakitic signature and can be compared with the subduction-related rocks with adakitic affinity described by Božović et al. (2013) in the Demir Kapija region (Fig. 7). The subvolcanic and volcanic rocks of Group 2b show some differences based on the sampling area (i.e., Demir Kapija and Lipkovo). The REE contents of CABs from Lipkovo are higher than those of Demir Kapija with ranges of La and Yb of 30-70 and 12-20 times chondrite (Sun and McDonough, 1989), respectively (Fig. 5f), likely indicating that the Lipkovo samples are more differentiated. The features of the Group 2b rocks suggest comparison with subduction-related rocks without adakitic affinity described by Božović et al. (2013).

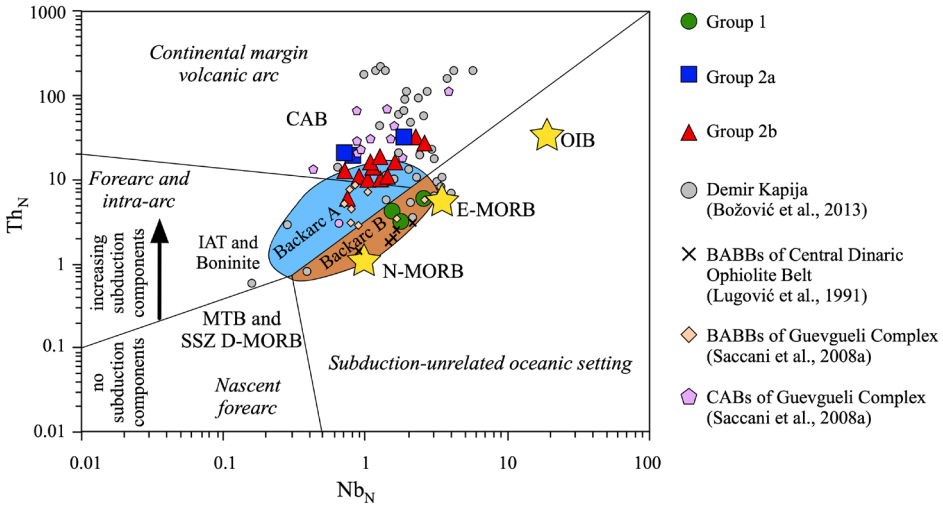

Fig. 6 - N-MORB normalized Nb vs. Th discrimination diagram of Saccani (2015) for subvolcanic and volcanic rocks of North Macedonia ophiolites. The compositions of backarc basin basalts and calc-alkaline basalts of the Guevgueli complex (Saccani et al., 2008b) and from Central Dinaric Ophiolite Belt (Lugović et al., 1991) are reported for comparison. Abbreviations, OIB: ocean island-type basalt; MORB: mid-ocean ridge basalt; N-: normal type; E-: enriched type; D-: depleted type; IAT: island arc tholeiite; CAB: calc-alkaline basalt; MTB: medium titanium basalt. Backarc A indicates BABB characterized by input of subduction or crustal components, whereas Backarc B indicates BABBs showing scarce input of subduction or crustal components. Normalizing values, as well as the composition of typical N-MORB, E-MORB, and OIB are from Sun and McDonough (1989).

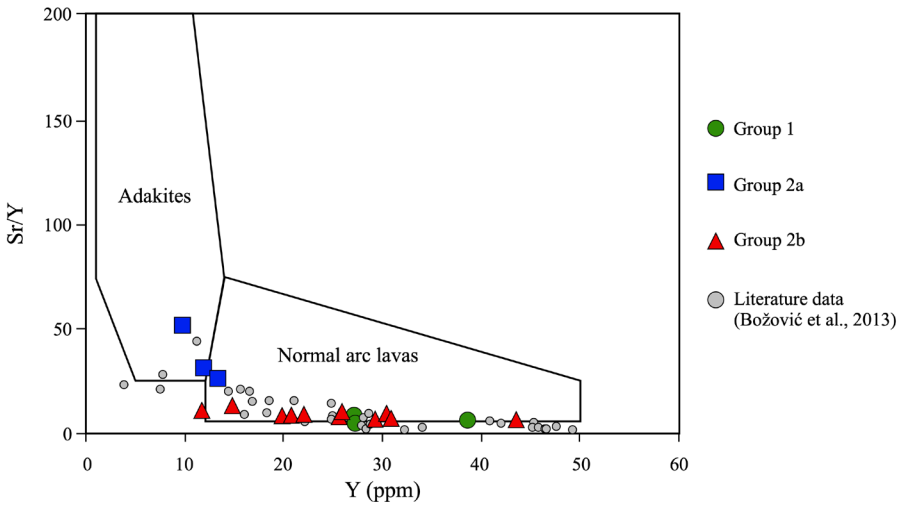

Fig. 7. Y vs. Sr/Y discriminating normal volcanic arc lavas from adakites for subvolcanic and volcanic rocks of North Macedonia ophiolites.

Carbon and sulphur isotopic composition

The C and S elemental contents and the respective isotopic ratios are reported in Table 2. The C contents of the North Macedonia ophiolites vary from very low (0.02 wt%) to relatively high (1.44 wt%) values. Also, the C isotopic composition ($\delta^{13}C$) encompass a wide range, from -22.9 to 0.4‰. Interestingly, the highest C contents are coupled with the least negative or the positive isotopic values, indicative of seafloor alteration with the presence of veins and/or vesicles filled with seawater carbonates, which are characterized by enriched C signature similar to that of the seawater (~ 0‰; Rollinson and Pease, 2021).

Table 2 - Elemental and isotopic compositions of carbon (C) and sulphur (S) in the subvolcanic and volcanic rocks of North Macedonia ophiolites.

	C (wt.%)	S (wt.%)	$\delta^{13}C_{(VPDB)}$ (‰)	$\delta^{34}S_{(VCDT)}$ (‰)
Subalkaline affinity				
Group 1				
DS13	0.10	<0.01	−10.6	2.4
DS14	0.04	<0.01	−22.8	0.7
DS15	0.03	<0.01	−16.7	0.7
Calc-alkaline affinity				
Group 2a				
DS7	0.87	<0.01	−0.4	−0.1
DS8	0.81	<0.01	−0.1	0.4
DS12	1.30	<0.01	0.3	3.1
Group 2b				
Demir Kapija				
DS3	1.17	<0.01	0.4	0.7
DS5	0.44	<0.01	−0.6	1.5
DS6	0.43	<0.01	−2.6	2.4
DS9	1.86	<0.01	−0.2	3.3
DS10	0.06	<0.01	−21.3	0.7
DS11	0.37	<0.01	−4.2	2.3
Lipkovo				
SL1	0.02	<0.01	−22.0	−0.7
SL2	0.03	<0.01	−22.9	2.5
SL3	1.44	<0.01	−11.5	3.3
SL4	0.04	<0.01	−22.2	3.2
SL5	0.02	<0.01	−18.2	4.9

For the Group 1 rocks, C contents are relatively low (0.03-0.10 wt%) and the isotopic composition of these samples is variable: two samples record isotopic values of -16.7‰ and -10.6‰, and one sample record a more negative isotopic value (-22.8‰). For Group 2a rocks, the C contents are relatively high (0.81-1.30 wt%) and they are coupled with less negative $\delta^{13}C$ values (from -0.4‰ to 0.3‰.), indicating the ubiquitous presence of secondary carbonates, which is confirmed by the petrographic observation and the XRD patterns. For Group 2b rocks, the C contents and $\delta^{13}C$ values are variable (from 0.02 wt% to 1.86 wt% and from -22.9‰ to 0.4‰, respectively). Therefore, in this group only some sample hosts secondary carbonates. Within the entire sample suite, excluding the rocks with high C contents and less negative $\delta^{13}C$, the samples display values that are isotopically more negative than the typical DMM and MORB signature (-5‰ ± 3; Cartigny et al., 2014; Fig. 8a), which suggest the input of fluids or melts with a different (more negative) C signature in the mantle source.

For S, all the investigated samples exhibit very low contents (< 0.01 wt%); nonetheless, reliable isotopic values ($\delta^{34}S$) were obtained (see Text 1S). On average, the rocks of Group 1 and Group 2a exhibit less positive isotopic values than those of Group 2b, where more samples exhibit S-enriched composition. However, it is important to note that the $\delta^{34}S$ values recorded by all the analyzed samples are isotopically more positive than those typical for DMM and MORB (-2.0 to -1.0‰ and -1.6 to -0.9‰, respectively; Rollinson and Pease, 2021), which suggest the involvement of fluids or melts with S-enriched composition.

DISCUSSION

Mantle sources of the North Macedonia ophiolites and metasomatizing slab-released components

According to the tectonic discrimination diagrams (Fig. 6), the Group 1 samples plot in the field for rocks from typical backarc basins, whereas those of Group 2 plot in the field for volcanic arc basalts. Therefore, the genesis of the North Macedonia ophiolites likely occurred in a SSZ setting, as previously suggested by Božović et al. (2013). In this tectono-magmatic environment, the genesis of volcanic rocks is

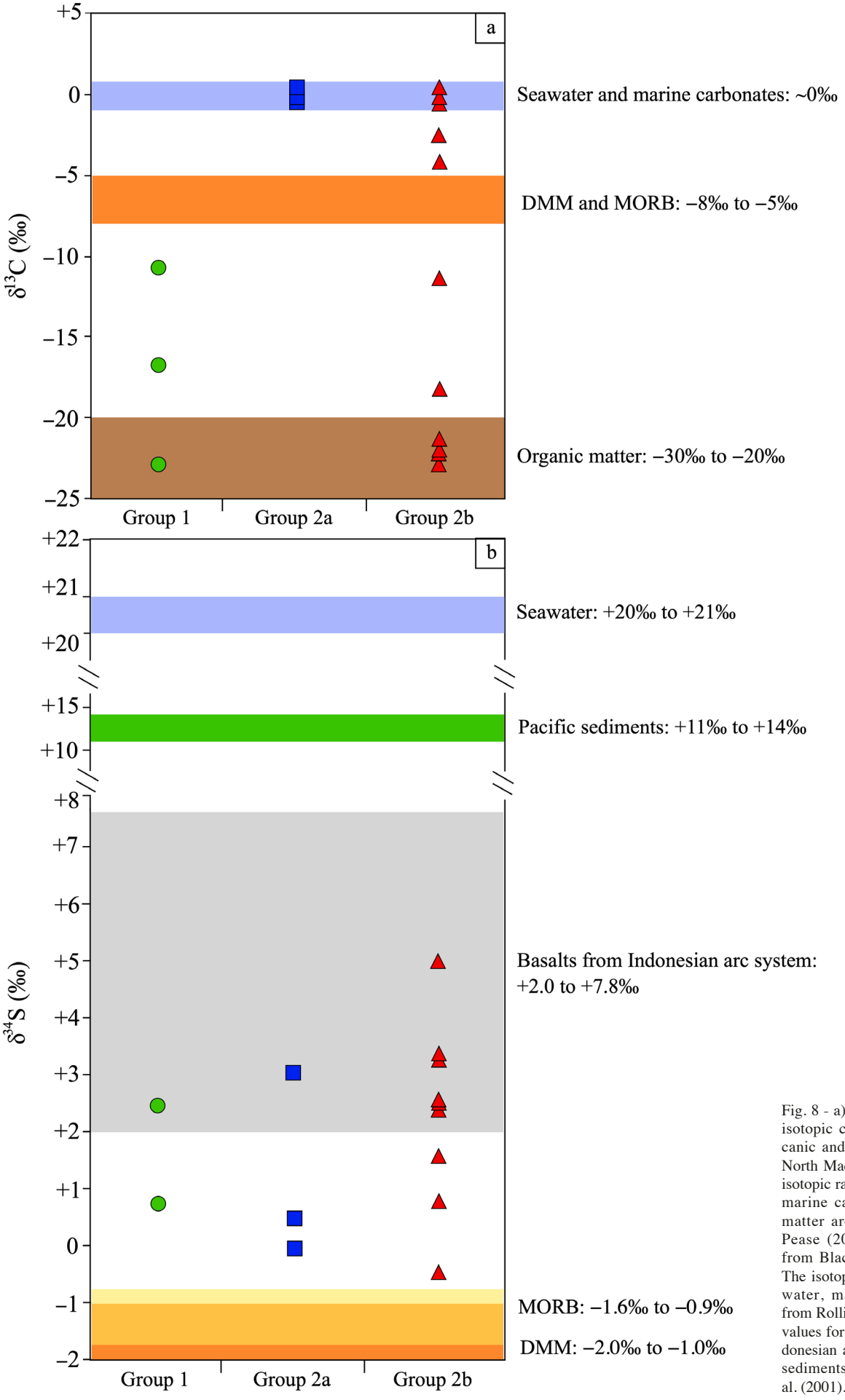

Fig. 8 - a) Carbon and b) sulphur isotopic composition of subvolcanic and volcanic rocks of the North Macedonia ophiolites. The isotopic ranges of C for seawater, marine carbonates and organic matter are from Rollinson and Pease (2021); mantle range is from Black and Gibson (2019). The isotopic ranges of S for seawater, mantle and MORB are from Rollinson and Pease (2021); values for basaltic rocks from Indonesian arc systems and Pacific sediments are from de Hoog et al. (2001).

classically related to the partial melting of subarc residual peridotites that experienced previous partial melting events followed by interaction with slab-derived fluids or melts that facilitate the hydrous partial melting of the peridotites (Pearce, 1983; Gribble et al., 1996; Parkinson and Pearce, 1998; Dilek and Furnes, 2011; Saccani et al., 2017).

To infer the mantle source composition of the North Macedonia ophiolites and the degree of partial melting we used a model based on the Cr vs Y covariation. Cr is a compatible trace element whose content is not significantly modified during the progressive mantle source depletion (i.e., progressive degree of partial melting), whereas Y is an incompatible trace element, whose abundance is closely related to source depletion and its degree of melting (Pearce, 1983). In addition, following Pearce (1983; 2014), Y behaves like a virtually immobile during the releasing of chemical components from the subducting slab. Therefore, the Cr vs Y model (Fig. 9) is not influenced by the nature and extent of chemical components released by the slab. In this model the possible mantle source compositions were chosen according to the SSZ chemical affinity of the studied rocks. In detail, three typical sub-arc mantle sources have been selected from Saccani et al. (2017): i) the slightly depleted lherzolite EP22 that represents residual mantle after ~ 12% MORB-type melt extraction; ii) the depleted lherzolite A19, which represents residual mantle after ~ 20% MORB-type melt extraction; iii) the strongly depleted lherzolite EP7 that represents residual mantle after ~ 12% MORB-type melt extraction followed by ~ 12% IAT-type melt extraction.

To evaluate the contribution of melts and aqueous fluids derived from subducted sediments to the mantle sources we used the Ba/Th vs Th/Nb plot (Fig. 10). Unfortunately, no constraints on the composition and nature of melts and aqueous fluids during the formation of the ophiolitic basalts are available. For this reason, we used the composition of the Average Serbian Flysch (ASF, Prelević et al., 2008) composed by sandstones and siltstones (Berisavljević et al., 2014) for the sediment melts, whereas the aqueous fluids are assumed as derived from the seawater (Li, 2000) interstitial in the sediments. The occurrence of rocks with adakitic signature in the North Macedonia ophiolites suggests that the contribution

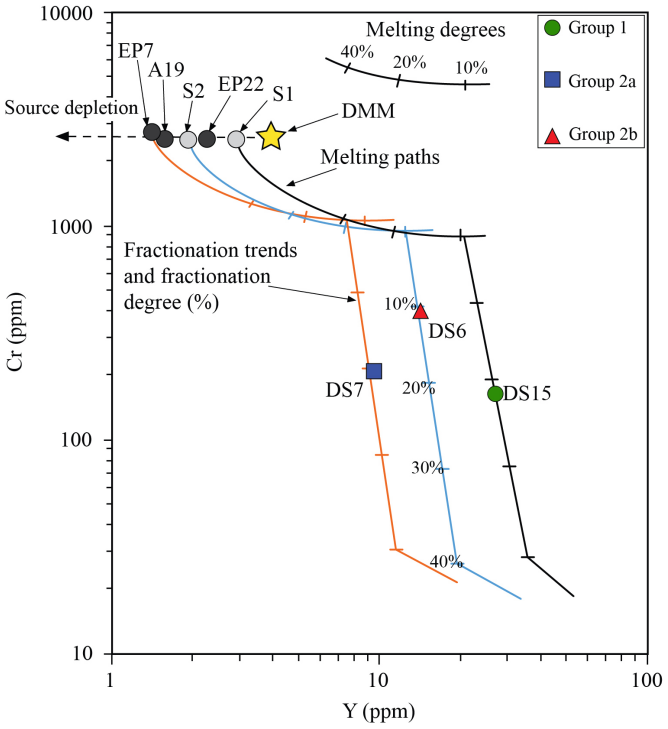

Fig. 9 - Y vs. Cr diagram of Pearce (1983) and melting models for subvolcanic and volcanic rocks of North Macedonia ophiolites. Abbreviations: DMM: depleted MORB mantle (Workman and Hart, 2005). Melting paths (with partial melting degrees) for incremental batch melting are calculated according to Murton (1989). In dark grey the composition of depleted mantle lherzolites assumed as possible mantle sources (EP7, A19, and EP22), from Saccani et al. (2017). Depleted lherzolites EP22 and A19 represent residual mantle after 12% and 20% MORB melt extraction from the DMM source, respectively; the depleted lherzolite EP7 represents residual mantle after 12% island arc tholeiitic melt extraction from a depleted mantle which is, in turn, residual after 12% MORB melt extraction from DMM. In light grey the composition of depleted mantle lherzolites calculated for this study and assumed as other possible mantle sources (S1 and S2). Depleted lherzolites S1 and S2 composition are intermediate between the DMM and EP22 and between EP22 and A19, respectively. The fractional crystallization trends are also shown (tick marks indicate 10% fractional crystallization steps).

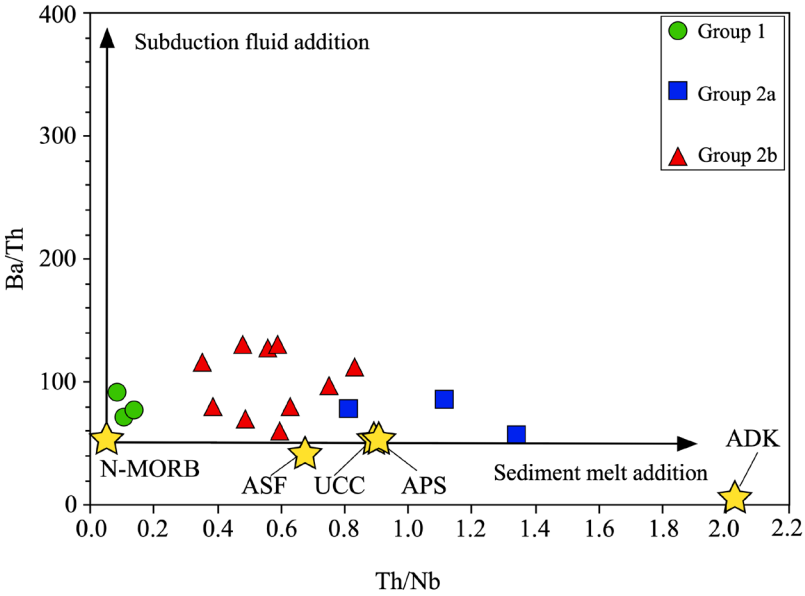

Fig. 10 - Ba/Th vs. Th/Nb diagram for subvolcanic and volcanic rocks from the North Macedonia ophiolites. The composition of normal-type mid-ocean ridge basalt (N-MORB), average Serbian flysch (ASF), upper continental crust (UCC); average pelitic sediments (APS); average adakitic component (ADK) are also shown. Data sources: N-MORB are from Sun and McDonough (1989); ASF are from Prelević et al. 2008; APS and UCC are from Taylor and McLennan (1985); ADK is calculated from 3% batch partial melting of an N-MORB eclogite with modal composition clinopyroxene = 0.5 and garnet = 0.5, and melting proportions clinopyroxene = 0.7 and garnet = 0.3. Partition coefficient for clinopyroxene and garnet are from Irving and Frey (1984).

of melts from the subducting oceanic crust must be considered (Fig. 10), as was already hypothesized by Božović et al. (2013) and observed in other volcanic arc assemblages worldwide (e.g., Defant and Drummond, 1990; Castillo, 2006; König et al., 2007; Barbero et al., 2020; Jentzer et al., 2020). This composition (Fig. 10) has been calculated assuming partial melting of an eclogite with whole rock composition of N-MORB of Sun and McDonough (1989).

For the Group 1 rocks, the sample DS15 (Mg# = 68.6) is assumed as the most primitive basalt The Cr-Y model suggests that it likely derived from ~ 8-10% partial melting of a theoretically calculated lherzolitic mantle source S1, whose composition is intermediate between DMM (Workman and Hart, 2005) and the slightly depleted EP22 (Fig. 9). The slight shifting of the Group 1 rocks from the typical MORB composition in Fig. 10 suggests that the mantle source composition was partially modified by chemical components released from the subducting slab. The relative enrichment of Ba/Th with respect to Th/Nb likely points out that the slab-released chemical components were predominantly composed of fluids rather than melts from the subducting sediment (Fig. 10).

For the Group 2a rocks, the most primitive basalt is represented by the DS7 (Mg# = 80.6). The Cr-Y model clearly indicate that the DS7 sample can be explained by ~ 12-15% partial melting of a mantle source that corresponds to a strongly depleted lherzolite (Fig. 9). The covariation of Ba/Th and Th/Nb ratios suggests that the EP7 source experience a relatively high degree of contamination from slab-released chemical components (Fig. 10). We assumed that these components correspond to melts derived from partial melting of subducting mafic crust (adakitic component, ADK) and subducting sediment melts like ASF (Prelević et al., 2008), similarly to what proposed by Božović et al. (2013).

For the Group 2b rocks, the DS6 sample (Mg# = 74.9) can be assumed as the most primitive basalt (Fig. 9). The Cr-Y model clearly indicates that the DS6 sample can be explained by ~ 10% partial melting of a theoretically calculated mantle source S2, whose composition is intermediate between the slightly depleted lherzolite EP22 and the depleted lherzolite A19 (Fig. 9). The composition of this source was likely modified prior to the melting event by the interaction with both aqueous fluid and sediment melts that have been released by the subducting slab (Fig. 10). In detail, the proportionally higher Th/Nb ratios with respect to the Ba/Th ratios likely suggest that the contribution from sediment melts was predominant.

Carbon and sulphur isotopes as proxies for slab-released components during subduction?

The subduction of sediments and altered oceanic lithosphere is the major process for the transfer of volatiles at the mantle depths relevant for arc magma genesis (Wallace, 2005; Zellmer et al.; 2015; Bekaert et al., 2021). Therefore, the volatiles' contents and fingerprints of SSZ rocks could theoretically be used to trace the subduction processes as well as to identify the nature of the volatile sources (Schwarzenbach, 2011; Alt et al., 2012; Schwarzenbach et al., 2018). However, other processes occurring in the mantle and at the crustal surface (e.g., fractionation, degassing, incorporation of sediments, seawater alteration) can mobilize C and S and consequently modify the original isotopic signature of the rocks. In the following sections the C and S fingerprints of the North Macedonia ophiolites were investigated to define the possible sources and processes responsible for the C and S fingerprints in the North Macedonia ophiolites.

Carbon isotopic fingerprint of the North Macedonia ophiolites

According to Deines (2002), the mean mantle value of $\delta^{13}C$ is ~ -5‰ (with an error of ±3 according to Cartigny et al., 2014). This value has been estimated by comparing isotopic measurements of diamonds, kimberlite xenoliths, carbonatites, MORBs, and OIBs. However, more negative $\delta^{13}C$ compositions were measured in eclogitic diamonds (-39 to -4‰, Deines et al., 2009; Shirey et al., 2013 and reference therein) and mantle peridotites (-18 to -15‰; Crespo et al., 2006; Bianchini and Natali, 2017). The potential causes of these "lighter" compositions (i.e., negative signature) is still matter of debate. They are attributed to features and processes occurring in the mantle: i) the heterogeneous nature of the mantle, which deviates locally from the "typical" mantle value (e.g., a ^{13}C-depleted mantle zone in Botswana; Deines et al., 2009); ii) the fractionation processes occurring in the mantle, as during partial melting ^{13}C is partitioned preferentially in fluids and the residual compositions have progressively more negative $\delta^{13}C$ values (Maruoka et al., 2004; Mizutani et al., 2014; Bianchini and Natali, 2017) and iii) the recycling in the mantle of organic carbon deriving from the subduction of seafloor sediments (Shirey et al., 2013 and reference therein; Cook-Kollars et al., 2014), as biological materials are strongly depleted in $\delta^{13}C$ (-30 to -20‰; Rollinson and Pease, 2021). Additionally, when magma erupts at the surface, other processes occurred in submarine and subaerial environments which could further modify the original C signatures of melts and igneous rocks. For example, during the ascent of magmas, CO_2 is exsolved from melt forming vesicles. The ^{13}C isotopes is partitioned preferentially in gaseous phases, so the C signature of CO_2 in vesicles is less negative than that of the residual CO_2 dissolved in the melt. As degassing progresses, the vesicles are removed therefore the residual lava assume more negative $\delta^{13}C$ values, which remain recorded in the derived igneous rocks (Aubaud et al., 2006; Barry et al., 2014; Bianchini and Natali, 2017). After the formation of the rocks, other processes could modify their C signature. In submarine environment the rocks could be affected by seafloor alteration, which generates secondary marine carbonates filling the fractures and vesicles of the rocks, characterized by enriched C signature similar to that of the seawater (~ 0‰; Rollinson and Pease, 2021). Furthermore, in subaerial environment the mafic and ultramafic rocks may interact with meteoric waters which dissolve primary Mg and Ca-bearing minerals like olivine and pyroxene and precipitate carbonate minerals as well as serpentine through low temperature serpentinization reactions. In particular case, like in Oman, hyperalkaline (pH > 11) groundwaters, which are produced by the modification of meteoric water infiltrating peridotites, can precipitate carbonates with very negative $\delta^{13}C$ values (~ -25‰) in the surface of ophiolites (Stephan, 2014).

The interplay of such various "deep" and "shallow" processes makes difficult to constrain the cause(s) responsible for the C isotopic fingerprint of volcanic and subvolcanic rocks, including those in the ophiolitic sequence. However, for the North Macedonia ophiolites we can tentatively make some inferences on the possible sources of C taking into account the petrographic observation, XRD patterns and chemical analyses, and the petrogenetic modeling. First of all, we identified the possible overprint by seafloor alteration, as the magma erupted in a submarine environment. Based on the petrographic observation and XRD patterns (Fig. 1S) calcite is present in the Group 2a (DS7, DS8, DS12) and in most Group 2b (DS3, DS5, DS6, DS9, DS11,

SL3) rocks. Accordingly, these samples have the highest contents of C coupled with the most enriched isotopic signatures (Table 2) within the sample suite, which reflect the imprint of seawater-derived carbonate rather than the pristine C composition of the rocks. Secondary carbonates are instead lacking in Group 1 (DS13, DS14, DS15) and in some Group 2b (DS10, SL1, SL2, SL4, SL5) samples, which show the lowest contents of C along with the most negative $\delta^{13}C$ values, far from the typical MORB range (-8 to -5‰; Marty and Zimmermann, 1999; Cartigny et al., 2001). Such features could be indicative of degassing processes and/or the presence of organic carbon in the mantle source released by the subducting sediments. We excluded the hypothesis of the incorporation of calcite with very negative C signature, as both the petrographic observation and XRD patterns revealed no trace of calcite in the rocks, and the samples have very lower C contents than what would be expected if secondary carbonates had been present.

The low C contents of these rocks also suggest that the magmas have degassed most of their C during the eruptions, thus allowing for C fractionation during CO_2 degassing. However, according to the REE petrogenetic modeling, small contributions of organic sediments are required in their mantle sources (Fig. 10). Therefore, it cannot be excluded that the negative C isotopic compositions could be also ascribed to the involvement of ^{13}C-depleted components, possibly in the form of terrigenous sediments containing organic matter. Most of the CABs of Groups 2a and 2b record more negative values respect to the BABBs of Group 1. Hence, we suggest that their mantle sources were closer to the subducting slab than those of the Group 1 and, consequently, they could be more affected by fluid and/or melt contamination.

Accordingly, the Group 1 of the North Macedonia shows a weak subduction signature in trace elements (Figs. 5a, b, 6), which means that the slab was relatively far from the spreading centre of the backarc basin and it weakly "contaminated" the mantle region with the released subduction fluids and melts. Therefore, the subduction-related signature was diluted in the MORB-like mantle region beneath the backarc basin. Similarly, the negative C isotopic signature of the slab-released components could be diluted in the ^{13}C-enriched MORB-like mantle region beneath the backarc basin. Thus, the $\delta^{13}C$ signature of the most of Group 1 rocks of the North Macedonia is slightly less negative than Groups 2a and 2b. Summarizing the variability of the C fingerprints among the rocks could be related to i) seawater alteration for the rocks of Group 2a and some rocks of Group 2b with C fingerprint close to 0‰, ii) degassing processes and/or iii) contamination of subducting sediments bearing C to the mantle sources for the Group 1 and Group 2b rocks having negative $\delta^{13}C$ values.

Sulphur isotopic fingerprint of the North Macedonia ophiolites

The S isotopic range of mantle is from -2.0‰ to -1.0‰ and for MORB is from -1.3‰ to -0.7‰ (Rollinson and Pease, 2021). Therefore, the isotopic values recorded by the North Macedonia ophiolites are more positive than the typical mantle and MORB signatures. These differences cannot be related to the fractionation processes of sulphur during the partial melting, as they are negligible according to Labidi and Cartigny (2016). The positive $\delta^{34}S$ values recorded in volcanic and subvolcanic rocks are generally associated to i) degassing processes (Hutchinson et al., 2019), ii) hydrothermal seawater alteration (Li et al., 2020; Burness et al., 2021) and/or iii) involvement of slab-material enriched in ^{34}S (Alt et al., 1993; de Hoog et al., 2001; Bénard et al., 2018; Walters et al., 2020). The North Macedonia ophiolites exhibit very low S contents (< 0.01 wt%), which could be indicative of degassing processes. However, according to Hutchinson et al. (2019) during degassing the $\delta^{34}S$ decreases in the residual melt. Also, the influence of hydrothermal seawater alteration seems unlikely, the rocks affected by this process should be characterized by higher sulphur contents and elevated $\delta^{34}S$ fingerprint close to the composition of water (e.g., see Alt and Shanks, 2003; Alt et al., 2007). On the other hand, according to the petrogenetic models of Figures 9 and 10, all the North Macedonia ophiolites originated from partial melting of subarc mantle sources metasomatized by variable proportion of melts from the subducting sediments. In general, the $\delta^{34}S$ composition of sediments is highly variable, depending on the relative amounts of sulphides and sulphates, which are characterized by strong negative and positive S fingerprints, respectively (de Hoog et al., 2001; Alt and Shanks, 2006; Schwarzenbach et al., 2018). Considering the positive $\delta^{34}S$ composition of the North Macedonia ophiolites, sulphate species should be predominant in the slab-sediments that metasomatized the mantle sources, similar to what suggested by de Hoog et al. (2001), who correlated the positive $\delta^{34}S$ values of basaltic rocks of Indonesian arc system (from 2.0 to 7.8‰) with the mixing of a depleted-S composition of pre-subduction mantle (~ 0‰) with enriched-S composition of the Pacific sediments (~ 12‰) (Fig. 8b).

Compared to C, the differences of isotopic S composition among the North Macedonia ophiolites are more evident. The S isotopic values of the Group 2b rocks are in general more positive than most of Group 1 and Group 2a rocks (Fig. 8b), reflecting different amounts of slab-released materials. This indicates that the Group 2b CABs were more affected by slab-derived melts than Group 1 BABBs. In fact, the mantle portion near the subducting slab is significantly affected by melts and fluids released from the subducting slab, and its original isotopic fingerprint is modified by the interaction with these components. Likewise, the Group 2b CABs record more enriched-S composition with respect to the Group 1 BABBs. However, also the $\delta^{34}S$ values of Group 1 BABBs are slightly positive and differ from the typical negative values of the DMM and MORBs (Fig. 8b), suggesting that their S isotope signatures result from mixing of MORB and subducting sediments. The CABs with adakitic signature (i.e., Group 2a) record slightly positive $\delta^{34}S$ values that are different from the CABs without adakitic signature (i.e., Group 2b). The reason for such difference is difficult to be clearly and univocally clarified. We suggest here that it may be related to a depleted S-isotopic composition of the adakitic melts, which metasomatized the mantle source. It appears that the signature of the adakitic melts is probably inherited by the melting of subducting oceanic crust components whose S composition could be similar to those of MOR-type basalts. However, it is important to note that the isotopic S composition of adakitic melts is still unknown in literature and further investigations to clearly prove this hypothesis worth to be done.

Tectono-magmatic significance and geodynamic implications

According to the new geochemical and C-S stable isotopic data, and the petrogenetic study, the North Macedonia ophiolites represent subduction-related ophiolites (according to the classification of Dilek and Furnes, 2011) which likely formed in an arc-backarc setting. The petrogenetic modeling and the

isotopic data show that this setting was characterized by different mantle sources and inputs of fluids and melts released from the subducting slab. The slab-released components appear limited in backarc setting where the Group 1 rocks were formed (Fig. 10). In line with this, the isotopic signature of the Group 1 rocks exhibits ^{13}C-enriched and ^{34}S-depleted signature, which indicates a scarce involvement of the subducting melts released from the sediments (Figs. 8a, b). Therefore, the petrogenetic processes in the backarc setting was likely dominated by the ascent of an asthenospheric mantle source showing MORB-mantle like composition (or slightly more depleted) and bearing diluted slab-released chemical components (Fig. 11). This is in accordance with Pearce et al. (2005), who predicted for the BABBs MORB-like patterns with weak subduction-related features as a consequence of either dispersed slab-released chemical components within the upwelling mantle materials or spreading centres distal from the subduction front. By contrast, in the volcanic arc setting, the ambient mantle sources correspond to strongly depleted peridotites, which underwent previous partial melting events and were strongly metasomatized by slab-released chemical components. Accordingly, C and S isotope signature of the volcanic arc rocks (i.e., Group 2 rocks) indicate the contributions of C-depleted and S-enriched components that fit with the typical signature of subducting sediments hosting organic matter and sulphate phases (Fig. 11). In addition, we hypothetically suggest that the depleted S isotopic composition of the Group 2a rock may be related to the involvement of melts from the subducting oceanic crust, which should bear isotopic signature comparable to those of typical MORB. Thus, our new data from the North Macedonia ophiolites suggest that the whole rock and C-S isotopic composition of subduction-related ophiolitic rocks is strongly dependent on the amount and type of slab-released chemical components and the distance from the subduction front (Fig. 11).

This conclusion is also significative for the geodynamic framework of the Dinaric-Hellenic belt. In fact, the supra-subduction signature found in North Macedonia ophiolites is recognizable in other ophiolites of the Vardar zone occurring in Albania (Bortolotti et al., 2013), Romania (Gallhofer et al., 2017), Serbia (Šarić et al., 2009), and Northern Greece (Zachariadis, 2007; Saccani et al.; 2008a). All these authors agreed that the Vardar ophiolites originated from Early to Late Jurassic in an arc-backarc setting related to the subducting Neotethys (see Boev et al., 2018 for a review). However, there are some different interpretations of the geodynamic setting of the southern Vardar zone ophiolites, i.e., the Demir Kapija and Guevgueli ophiolites (Saccani et al., 2008a; Fig. 5a, b). According to Bozović et al. (2013), the Demir Kapija-Guevgueli complex formed in an oceanic backarc basin after the slab roll-back behind the Paikon arc, an immature island arc. On the other hand, Bébien et al. (1986) and Saccani et al. (2008a) proposed that the Guevgueli ophiolites formed in an ensialic backarc basin developed between the continental margin of the Serbo-Macedonian Massif and that the Paikon arc represented a volcanic arc with calc-alkaline magmatism, emplaced in the European continental lithosphere and split off from the European margin. The new data on the North Macedonia ophiolites agree with the scenario of an ensialic backarc basin. The occurrence of ophiolitic rocks with calc-alkaline affinity in Lipkovo and Demir Kapija areas suggests the existence of a magmatic arc, likely representing the prosecution of the Paikon arc. In addition, the close association of coeval BABB and CAB rocks in the Demir Kapija-Guevgueli complex supports an ensialic backarc setting rather than an intraoceanic backarc which is commonly characterized by magmatism with island arc tholeiitic and boninitic affinity (e.g., Dilek, 2003; Pearce et al., 2005; Whattam and Stern, 2011; Saccani et al., 2011; 2017; Maffione and Van Hinsenbergen, 2018).

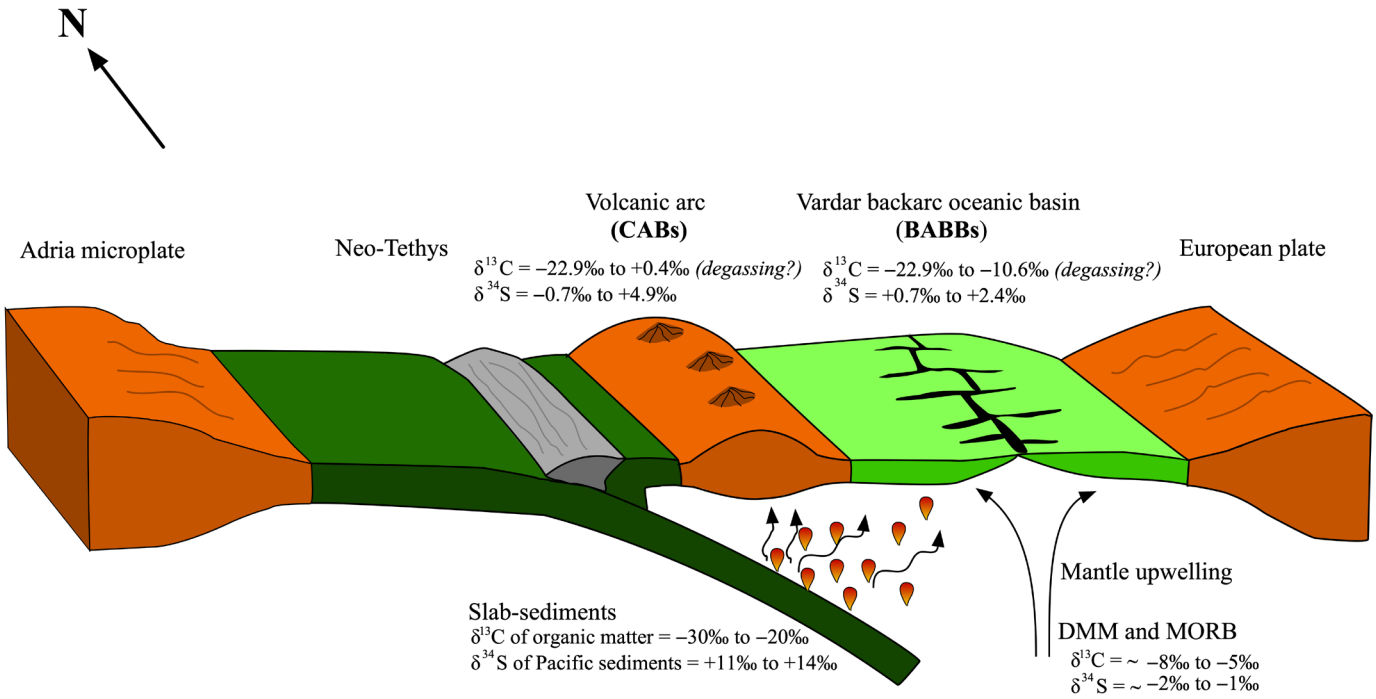

Fig. 11. Schematic cartoon (not to scale) showing the different contribution of slab-released components (melts from both sediments and oceanic crust) to the backarc basin basalts (BABB) and calc-alkaline (CAB) rocks of the North Macedonia ophiolites during Middle - Late Jurassic times.

CONCLUSIONS

The Vardar zone ophiolites of North Macedonia consist of MOR-type basalt formed in backarc basin and calc-alkaline basalts. According to trace elements and rare earth element contents and patterns, these rocks represent subduction-related ophiolites formed in different tectonic settings: backarc basins, together with those of the near Guevgueli complex in the Northern Greece, and volcanic arcs. According to the Cr vs Y and Ba/Th vs Th/Nb models the magmatic rocks of the North Macedonia ophiolites invariably formed by mantle sources variably metasomatized by subduction-related components, including sediment melts and, locally, adakitic melts. Subduction components contaminated the mantle sources to different extent, with a smaller contribution in the backarc basin basalt mantle source rather than in the calc-alkaline mantle source. The carbon (C) and sulphur (S) isotopic composition seems to reflect the slab-contamination, as all the North Macedonia ophiolites have isotopic signature which deviated from those typical for mantle and Mid Ocean Ridge melts. The negative C signatures of volcanic and subvolcanic products could be attributed to the involvement of slab lithospheric components dragged in the mantle, such as sediments with ^{13}C-depleted organic matter. On the other hand, this could also be an effect of C fractionation due to degassing processes during the eruptions. For S, the positive isotopic signatures of the North Macedonia ophiolites indicates that the mantle source were affected by ^{34}S-enriched melts derived from the subducting sediments with sulphate-bearing phases. In particular, the Group 2b rocks record more positive $\delta^{34}S$ values than the subalkaline basalts of Group 1 formed in backarc basin suggesting that the influence of the volatiles depends on the distance of the mantle sources from the arc as the mantle regions near to subducting slab are more metasomatized than those far away from the trench. Therefore, this work shows that research on stable isotopes, especially S, in volcanic and subvolcanic rocks from different geological settings should be improved in order to investigate the sources and the pathways of volatiles in subduction zone.

ACKNOWLEDGEMENTS

The research has been funded by: CEI-KEP project (Ref. No. 1206.006-19) Geccospark Project titled "*Promoting geological, ecological and cultural heritage through sustainable development and creation of geo-parks*" (Head G. B.), FAR-2018 Project of the Ferrara University (Head E.S.). Maurizio Mazzucchelli (University of Modena and Reggio Emilia) and Renzo Tassinari (University of Ferrara) are acknowledged for technical support with geochemical analysis, Marcello Serracino (CNR-IGAG, Rome) and Valentina Corti (Se.So.Lab.) are acknowledged for EMPA analysis and thin section production, respectively. The authors thank Dejan Prelević, Osman Parlak, and an anonymous reviewer for their informative and constructive reviews, as well as Alessandra Montanini for the editorial handling.

REFERENCES

Alt J.C. and Shanks W.C., 2003. Serpentinization of abyssal peridotites from the MARK area, Mid-Atlantic Ridge: sulfur geochemistry and reaction modeling. Geochim. Cosmochim. Acta, 67: 641-653.

Alt J.C. and Shanks W.C., 2006. Stable isotope compositions of serpentinite seamounts in the Mariana Forearc: serpentinization processes, fluid sources and sulfur metasomatism. Earth Planet. Sci. Lett., 242: 272-285.

Alt J.C., Garrido C.J., Shanks W.C., Turchyn A., Padrón-Navarta A., Sánchez-Vizcaíno V.L., Gómez Pugnaire M.T.and Marchesi C., 2012. Recycling of water, carbon, and sulfur during subduction of serpentinites: a stable isotope study of Cerro del Almirez, Spain. Earth Planet. Sci. Lett., 327-328: 50-60.

Alt J.C., Shanks III W.C., Bach W., Paulick H., Garrido C.J. and Beaudoin G., 2007. Hydrothermal alteration and microbial sulfate reduction in peridotite and gabbro exposed by detachment faulting at the Mid-Atlantic Ridge, 15 20'N (ODP Leg 209): a sulfur and oxygen isotope study. Geochem. Geophy. Geosyst., 8 (8): Q08002.

Alt J.C., Shanks W.C. and Jackson M.C., 1993, Cycling of sulfur in subduction zones: the geochemistry of sulfur in the Mariana-island arc and back-arc trough. Earth Planet. Sci. Lett., 119: 477-494.

Aubaud C., Pineau F., Hékinian R. and Javoy M., 2006. Carbon and hydrogen isotope constraints on degassing of CO2 and H2O in submarine lavas from the Pitcairn hotspot (South Pacific). Geophys. Res. Lett. 33 (2): L02308.

Augé T., Morin G., Bailly L. and Serafimovsky T., 2017. Platinum-group minerals and their host chromitites in Macedonian ophiolites. Eur. J. Miner., 29: 585-596.

Barbero E., Delavari M., Dolati A., Saccani E., Marroni M., Catanzariti R. and Pandolfi L., 2020. The Ganj Complex reinterpreted as a Late Cretaceous volcanic arc: implications for the geodynamic evolution of the North Makran domain (southeast Iran). J. Asian Earth Sci., 195: 104306.

Barry P.H., Hilton D.R., Füri E., Halldórsson S.A. and Grönvold K., 2014. Carbon isotope and abundance systematics of Icelandic geothermal gases, fluids and subglacial basalts with implications for mantle plume-related CO_2 fluxes. Geochim. Cosmochim. Acta, 134: 74-99.

Bébien J., Dimo-Lahitte A., Vergély P., Insergueix-Filippi D. and Dupeyrat L., 2000. Albanian Ophiolites. I - Magmatic and metamorphic processes associated with the initiation of a subduction. Ofioliti, 25: 47-53.

Bébien J., Dubois R. and Gauthier A., 1986. Example of ensialic ophiolites emplaced in a wrench zone; innermost Hellenic ophiolite belt (Greek Macedonia). Geology, 14: 1016-1019.

Beccaluva L., Bianchini G., Natali C. and Siena F., 2017. The alkaline-carbonatite complex of Jacupiranga (Brazil): Magma genesis and mode of emplacement. Gondw. Res., 44: 157-177.

Beccaluva L., Coltorti M., Premti I., Saccani E., Siena F. and Zeda O., 1994. Mid-Ocean Ridge and Suprasubduction affinities in the Ophiolitic Belts from Albania. In: L. Beccaluva (Ed.), Albanian ophiolites: State of the art and perspectives. Ofioliti, 19: 77-96.

Beccaluva L., Macciotta G., Piccardo G.B. and Zeda O., 1989. Clinopyroxene compositions of ophiolite basalts as petrogenetic indicator. Chem. Geol., 77: 165-182.

Berisavljević Z., Berisavljević D. and Čebašek V., 2014. Shear strength properties of Dimitrovgrad flysch, Southeastern Serbia. Bull. Eng. Geol. Environ., 74: 759-773.

Bekaert D.V., Turner S.J., Broadley M.W., Barnes J.D., Halldórsson S.A., Labidi J., Wade J., Walowski K.J. and Barry P.H., 2021. Subduction-driven volatile recycling: a global mass balance. Annu. Rev. Earth Planet. Sci., 49: 37-70.

Bénard A., Klimm K., Woodland A.B., Arculus R.J., Wilke M., Botcharnikov R.E., Shmizu N., Nebel O., Rivard C. and Ionov D.A., 2018. Oxidising agents in sub-arc mantle melts link slab devolatilization and arc magmas. Nat. Commun., 9: 3500.

Bianchini G. and Natali C., 2017. Carbon elemental and isotopic composition in mantle xenoliths from Spain-Insights on sources and petrogenetic processes. Lithos, 272-273: 84-91.

Black B.A. and Gibson S.A., 2019. Deep Carbon and the life cycle of Large Igneous Province. Elements, 15: 319-324.

Boev B., Cvetković V., Prelević D., Šarić K. and Boev I., 2018. East Vardar ophiolites revisited: a brief synthesis of geology and geochemical data. Contribut. Sect. Nat. Math. Biotech. Sci. MASA, 39 (1): 51-68.

Bortolotti V., Chiari M., Marroni M., Pandolfi L., Principi G. and Saccani E., 2013. Geodynamic evolution of ophiolites from Albania and Greece (Dinaric-Hellenic belt): One, two, or more oceanic basins? Int. J. Earth Sci., 102 (3): 783-811.

Božović M., Prelević D., Romer R.L., Barth M., van den Bogaard P. and Boev B., 2013. The Demir Kapija Ophiolite, Macedonia (FYROM): a snapshot of subduction initiation within a back-arc. J. Petrol., 54 (7): 1427-1453.

Burness S., Thomassot E., Smart K.A. and Tappe S., 2021. Sulphur isotopes ($\delta^{34}S$ and ^{33}S) in sulphides from cratonic mantle eclogites: Aglimpse of volatile cycling in ancient subduction zones. Earth Planet. Sci. Lett., 572, 117118.

Burns L.E., 1985. The Border Ranges ultramafic and mafic complex, south-central Alaska: Cumulate fractionates of island-arc volcanics. Can. J. Earth Sci., 22: 1020-1038.

Cann J.R., 1970. Rb, Sr, Y, Zr and Nb in some ocean floor basaltic rocks. Earth Planet. Sci. Lett., 10: 7-11.

Cartigny P., Jendrzejewski N., Pineau F., Petit E. and Javoy M., 2001. Volatile (C, N, Ar) variability in MORB and the respective roles of mantle source heterogeneity and degassing: the case of the Southwest Indian Ridge. Earth Planet. Sci. Lett., 194: 241-257.

Cartigny P., Palot M., Tnomassot E. and Harris J.W., 2014. Diamond formation: A stable isotope perspective. Annu. Rev. Earth Planet. Sci., 42: 699-732.

Castillo P.R., 2006. An overview of adakite petrogenesis. Chin. Sci. Bull., 51 (3): 257-268.

Chiari M., Djeric´ N., Garfagnoli F., Hrvatovic H., Krstiç M., Levi N., Malasoma A., Marroni M., Menna F., Nirta G., Pandolfi L., Principi G., Saccani E., Stojadinoviç U. and Triviç B., 2011. The geology of the Zlatibor-Maljen area (Western Serbia): A geotraverse across the Dinaric-Hellenic collisional belt. Ofioliti, 36: 139-166.

Cook-Kollars J., Bebout G.E., Collins N.C., Angiboust S. and Agard P., 2014. Subduction zone metamorphic pathway for deep carbon cycling: I. Evidence from HP/UHP metasedimentary rocks, Italian Alps. Chem. Geol., 386: 31-48.

Coplen T.B. and Qi H., 2011. USGS42 and USGS43: Human-hair stable hydrogen and oxygen isotopic reference materials and analytical methods for forensic science and implications for published measurement results. Forensic Sci. Int., 214: 1-3.

Crespo E., Lique F.J., Rodas M., Wada H. and Gervilla F., 2006. Graphite-sulfide deposits in Ronda and Beni Bousera peridotites (Spain and Morocco) and the origin of carbon in mantle derived rocks. Gondw. Res., 9: 279-290.

de Hoog J.C.M., Taylor B.E. and van Bergen M.J., 2001. Sulfur isotope systematics of basaltic lavas from Indonesia: implications for the sulfur cycle in subduction zones. Earth Planet. Sci. Lett., 189: 237-252.

Defant M.J. and Drummond M.S., 1990. Derivation of some modern arc magms by melting of young lithosphere. Nature, 347: 662-665.

Deines P., 2002. The carbon isotope geochemistry of mantle xenoliths. Earth Sci. Rev., 58: 247-278.

Deines P., Stachel T. and Harris J.W., 2009. Systematic regional variations in diamond carbon isotopic compositions and inclusion chemistry beneath the Orapa kimberlite cluster in Botswana. Lithos, 112: 776-784.

Dilek Y., 2003. Ophiolite concept and its evolution. In: Y. Dilek and S. Newcomb (Eds.), Ophiolite concept and the evolution of geological thought. Geol. Soc. Am. Spec. Pap., 373: 1-16.

Dilek Y. and Furnes H., 2011. Ophiolite genesis and global tectonics: geochemical and tectonic fingerprinting of ancient oceanic lithosphere. Geol. Soc. Am. Bull., 123 (3/4): 387-411.

Dilek Y. and Furnes H., 2014. Ophiolites and their origins. Elements, 10: 93-100.

Dilek Y., Furnes H. and Shallo M., 2007. Suprasubduction zone ophiolite formation along the periphery of Mesozoic Gondwana. Gondw. Res., 11: 453-475.

Ferrière J., Chanier F. and Ditbanjong P., 2012. The Hellenic ophiolites: eastward or westward obduction of the Maliac Ocean, a discussion. Int. J. Earth Sci. (Geol Rundsch), 101: 1559-1580.

Franzini M., Leoni L. and Saitta M., 1975. Revisione di una metodologia analitica per Fluorescenza-X, basata sulla correzione completa degli effetti di matrice. Rend. Soc. It.. Miner. Petrol., 31: 365-378.

Furnes H., Dilek Y., Zhao G., Safanova I. and Santosh M., 2020. Geochemical characterization of ophiolites in the Alpine-Himalayan Orogenic Belt: Magmatically and tectonically diverse evolution of the Mesozoic Neotethyan oceanic crust. Earth Sci. Rev., 208: 103258.

Gallhofer D., von Quadt A., Schmid S.M., Guillong M., Peytcheva I. and Seghedi I., 2017. Magmatic and tectonic history of Jurassic ophiolites and associated granitoids from the South Apuseni Mountains (Romania). Swiss J. Geosci., 110: 699-719.

Gribble R.F., Stern R.J., Bloomer S.H., Stuben D., O'Hearn T. and Newman S., 1996. MORB mantle and subduction components interact to generate basalts in the southern Mariana Trough back-arc basin. Geochim. Cosmochim. Acta, 60: 2153-2166.

Gurenko A.A., Trumbull R.B., Thomas R. and Linsday J.M., 2005. A melt inclusion record of volatiles, trace elements and Li-B isotope variations in a single magma system from the Plat Pays Volcanic Complex, Dominica, Lesser Antilles. J. Petrol., 46: 2495-2526.

Halas S. and Szaran J., 2001. Improved thermal decomposition of sulfates to SO_2 and mass spectrometric determinations of $\delta^{34}S$ of IAEA-SO-5, IAEA-SO-6 and NBS-127 sulfate standards. Rapid Commun. Mass Spectrom., 15: 1618-1620.

Hébert R. and Laurent R., 1990. Mineral chemistry of the plutonic section of the Troodos ophiolite: New constraints for genesis of arc-related ophiolites. In: J. Malpas, E. Moores, A. Panayiotou and C. Xenophontos (Eds.). Troodos Ophiolite Symp., Ministry Agric. Natural Res., Geol. Survey Dept, Nicosia, Cyprus, p. 149-163.

Hutchinson W., Babiel R.J., Finch A.A., Marks M.A.W., Markl G., Boyce A.J., Stüeken E.E., Friis H., Borst A.M. and Horsburgh N.J., 2019. Sulphur isotopes of alkaline magmas unlock long-term records of crustal recycling on Earth. Nat. Comm., 10: 4208.

Irving, A.J. and Frey, F.A., 1984. Trace element abundances in megacrysts and their host basalts: constraints on partition coefficients and megacryst genesis. Geochim. Cosmochim. Ac. 48, 1201-1221.

Jentzer M., Whitechurch H., Agard P., Ulrich M., Caron B., Zarrinkoub M.H., Kohansal R., Miguet L., Omrani J. and Fournier M., 2020. Late Cretaceous calc-alkaline and adakitic magmatism in the Sistan suture zone (Eastern Iran): implications for subduction polarity and regional tectonics. J. Asian Earth Sci., 204 (2): 104588.

Karamata S., 2006. The geological development of the Balkan Peninsula related to the approach, collision and compression of Gondwanan and Eurasian units. In: A.H.F. Robertson, D. Mountrakis (Eds.). Tectonic development of the Eastern Mediterranean region, Geol. Soc. Spec. Publ. London, 260 (1), p. 155-178.

Kilias A., Frisch W., Avgerinas A., Dunkl I., Falalakis G. and Gawlick H.-J., 2010. Alpine architecture and kinematics of deformation of the northern Pelagonian nappe pile in the Hellenides. Austrian J. Earth Sci., 103: 4-28.

König S., Schuth S., Munker C. and Qopoto C., 2007. The role of slab melting in the petrogenesis of high-Mg andesites: evidence from Simbo Volcano, Solomon Islands. Contrib. Miner. Petrol., 153: 85-103.

Kukoč D., Goričan Š., Košir A., Belak M., Halamić J. and Hrvatović H., 2015. Middle Jurassic age of basalts and the post-obduction sedimentary sequence in the Guevgueli Ophiolite Complex (Republic of Macedonia). Int. J. Earth Sci., 104 (2): 435-447.

Labidi J. and Cartigny P., 2016. Negligible sulfur isotope fractionation during partial melting: Evidence from Garrett transform fault basalts, implications for the late-veneer and the Hadean matte. Earth Planet. Sci. Lett., 451: 196-207.

Leoni L. and Saitta M., 1976. X-ray Fluorescence analysis of 29 trace elements in rock and mineral standards. Rend. Soc. It. Miner. Petrol., 32: 497-510.

Leterrier J., Maury R.C., Thonon P., Girard D. and Marchal M., 1982. Clinopyroxene composition as a method of identification of the magmatic affinities of paleo-volcanic series. Earth Planet. Sci. Lett., 59: 139-154.

Li Y.H., 2000. A compendium of geochemistry: from solar nebula to the human brain. Princeton Univ. Press, Princeton, NJ. 440 pp.

Li J.-L., Klemd R., Huang G.-F., Ague J.J. and Gao J., 2020. Unravelling slab $\delta^{34}S$ compositions from in-situ sulphide δ34S studies of high-pressure metamorphic rocks. Int. Geol. Rev., 10.1080/00206814.2020.1827305.

Li J.-L., Schwarzenbach E.M., John T., Ague J.J., Tassara S., Gao J. and Konecke B.A., 2021. Subduction zone sulfur mobilization and redistribution by intraslab fluid-rock interaction. Geochim. Cosmochim. Acta, 297: 40-64.

Lugović B., Altherr R., Raczek I., Hofmann A.W. and Majer V., 1991. Geochemistry of peridotites and mafic igneous rocks from the Central Dinaric Ophiolite Belt, Yugoslavia. Contrib. Miner. Petrol., 106 (2): 201-216.

Maffione M. and van Hinsenbergen D.J.J., 2018. Reconstructing plate boundaries in the Jurassic Neo-Tethys from the East and West Vardar ophiolites (Greece and Serbia). Tectonics, 37: 858-887.

Marty B. and Zimmermann L., 1999. Volatiles (He, C, N, Ar) in mid-ocean ridge basalts: assessment of shallow-level fractionation and characterisation of source composition. Geochim. Cosmochim. Acta, 63: 3619-3633.

Maruoka T., Kurat G., Dobosi G. and Koeberl C., 2004. Isotopic composition of carbon in diamonds of diamondites: record of mass fractionation in the upper mantle. Geochim. Cosmochim. Acta, 68: 1635-1644.

Mercier J., 1966. Mouvements orogéniques et magmatisme d'age Jurassique Supérieur-Éocrétacé dans les Zones Internes des Hellénides (Macédoine, Grèce). Rev. Géogr. Phys. Géol. Dynam., 8: 265-278

Mizutani S., Satish.Kumar M. and Yoshino T., 2014. Experimental determination of carbon isotope fractionation between graphite and carbonated silicate melt under upper mantle conditions. Earth Planet. Sci. Lett., 392: 86-93.

Murton B.J., 1989. Tectonic controls on boninite genesis. In: A.D. Saunders, M.J. Norry (Eds.). Magmatism in the ocean basins. Geol. Soc. Spec. Publ. London, 42 (1), p. 347-377.

Natali C. and Bianchini G., 2015. Thermally based isotopic speciation of carbon in complex matrices: a tool for environmental investigation. Environ. Sci. Pollut. Res., 22: 12162-12173.

Pamić J., 2002. The Sava-Vardar Zone of the Dinarides and Hellenides versus the Vardar Ocean. Ecl. Geol. Helv., 95: 99-113.

Parkinson I.J. and Pearce J.A., 1998. Peridotites from the Izu-Bonin-Mariana forarc (ODP Leg 125): evidence for mantle melting and melt-mantle interaction in a suprasubduction zone setting. J. Petrol., 39: 1577-1618.

Parlak O., Bağcı U., Rızaoğlu T., Ionescu C., Önal G., Höck V. and Kozlu H., 2020. Petrology of ultramafic to mafic cumulate rocks from the Göksun (Kahramanmaraş) ophiolite, southeast Turkey. Geosci. Front, 11 (1): 109-128.

Pearce J.A., 1982. Trace element characteristics of lavas from destructive plate boundaries. In: R.S. Thorpe (Ed.), Andesites. Wiley and Sons, New York, p. 525-548.

Pearce J.A., 1983. Role of the sub-continental lithosphere in magma genesis at active continental margin. In: C.J. Hawkesworth and M.J. Norry (Eds.), Continental basalts and mantle xenoliths. Shiva, Nantwich, p. 230-249.

Pearce J.A., 2014. Immobile element fingerprinting of ophiolites. Elements, 10 (2): 101-108.

Pearce J.A. and Norry M.J., 1979. Petrogenetic implications of Ti, Zr, Y, and Nb variations in volcanic rocks. Contrib. Miner. Petrol., 69: 33-47.

Pearce J.A., Stern R.J., Bloomer S.H. and Fryer P., 2005. Geochemical mapping of the Mariana arc-basin system: Implications for the nature and distribution of subduction components. Geochem. Geophy. Geosyst., 6 (7): Q07006.

Pe-Piper G. and Piper D.J.W., 2002. The igneous rocks of Greece. The anatomy of an orogen. Gebrueder Borntraeger, Berlin, 573 pp.

Petrušev E., Stolić N., Šajn R. and Stafilov T., 2021. Geological characteristics of the Republic of North Macedonia. Geol. Maced., 35 (1): 49-58.

Prelević D., Foley S.F., Romer R. and Conticelli S., 2008. Mediterranean Tertiary lamproites derived from multiple source components in postcollisional geodynamics. Geochim. Cosmochim. Acta, 72: 2125-2156.

Robertson A.H.F., 2002. Overview of the genesis and emplacement of Mesozoic ophiolites in the Eastern Mediterranean Tethyan region. Lithos, 65 (1-2): 1-67.

Robertson A.H.F. and Shallo M., 2000. Mesozoic-Tertiary tectonic evolution of Albania in its regional Eastern Mediterranean context. Tectonophysics, 316 (3-4): 197-254.

Robertson A.H.F., Karamata S. and Šarić K., 2009. Ophiolites and related geology of the Balkan region. Lithos, 108: 1-36.

Rollinson H. and Pease V., 2021. Using stable isotope data. In: Using geochemical data: to understand geological processes. Cambridge Univ. Press, p. 219-285.

Ruth D.C.S., Costa F., Bouvet de Maisonneuve C., Franco L., Cortés J.A. and Calder E.S., 2018. Crystal and melt inclusion timescales reveal the evolution of magma migration before eruption. Nat. Commun., 9: 2657.

Saccani E., 2015. A new method of discriminating different types of post-Archean ophiolitic basalts and their tectonic significance using Th-Nb and Ce-Dy-Yb systematics. Geosci. Front., 6: 481-501.

Saccani E., Beccaluva L., Photiades A. and Zeda O., 2011. Petrogenesis and tectono-magmatic significance of basalts and mantle peridotites from the Albanian-Greek ophiolites and sub-ophiolitic mélanges. New constraints for the Triassic-Jurassic evolution of the Neo-Tethys in the Dinaride sector. Lithos, 124: 227-242.

Saccani E., Bortolotti V., Marroni M., Pandolfi L., Photiades A. and Principi G., 2008a. The Jurassic association of backarc basin ophiolites and calc-alkaline volcanics in the Guevgueli complex (Northern Greece): implications for the evolution of the Vardar Zone. Ofioliti, 33 (2): 209-227.

Saccani E., Chiari M., Bortolotti V., Photiades A. and Principi G., 2015. Geochemistry of volcanic and subvolcanic rocks and biostratigraphy on radiolarian cherts from the Almopias ophiolites and Paikon unit (Western Vardar, Greece). Ofioliti, 40: 1-25.

Saccani E., Dilek Y. and Photiades A., 2017. Time-progressive mantle-melt evolution and magma production in a Tethyan marginal sea: a case study of the Albanide-Hellenide ophiolites. Lithosphere, 10: 35-53.

Saccani E., Photiades A., Santato A. and Zeda O., 2008b. New evidence for supra-subduction zone ophiolites in the Vardar zone from the Vermion massif (northern Greece): Implication for the tectono-magmatic evolution of the Vardar oceanic basin. Ofioliti, 33: 65-85.

Šarić K., Cvetković V., Romer R.L., Christofides G. and Koroneos A., 2009. Granitoids associated with East Vardar ophiolites (Serbia, F.Z.R. of Macedonia and Northern Greece): origin, evolution and geodynamic significance inferred from major and trace element data and Sr-Nd-Pb isotopes. Lithos, 108 (1-4): 131-150.

Schmid S.M., Bernoulli D., Fügenschuh B., Matenco L., Schefer S., Schuster R., Tischler M. and Ustaszewski K., 2008. The Alpine-Carpathian-Dinaridic orogenic system: correlation and evolution of tectonic units. Swiss J. Geosci., 101: 139-183.

Schwarzenbach E., 2011. Serpentinization, fluids and life: comparing carbon and sulfur cycles in modern and ancient environments, PhD Thesis, ETH Zurich, 194 pp.

Schwarzenbach E.M., Caddick M.J., Petroff M., Gill B.C., Cooperdock E.H. and Barnes J.D., 2018. Sulphur and carbon cycling in the subduction zone mélange. Sci. Rep., 8:15517.

Sharp I. and Robertson A., 1994. Late Jurassic - Lower Cretaceous oceanic crust and sediments of the eastern Almopias Zone, NW Macedonia (Greece); implications for the evolution of the eastern "Internal" Hellenides. Bull. Geol. Soc. Greece, 30: 47-61.

Shirey S.B., Cartigny P., Frost D.J., Keshav S., Nestila F., Nimis P., Pearson D.G., Sobolev N.V. and Walter M.J., 2013. Diamonds and the geology of mantle carbon. Rev. Miner. Geochem., 75: 355-421.

Smith A.G., 1993. Tectonic significance of the Hellenic-Dinaric ophiolites. In: H.M. Prichard, T. Alabaster, N.B.W. Harris, C.R. Neary (Eds.). Magmatic processes and plate tectonics. Geol. Soc. Spec. Publ. London, 76, p. 213-243.

Šoster A., Zavašnik J., O'Sullivan P., Herlec U., Potočnik Krajnc B., Palinkaš L., Zupančič N. and Dolenec M., 2020. Geochemistry of Bashibos-Bajrambos metasedimentary unit, Serbo- Macedonian massif, North Macedonia: Implications for age, provenance and tectonic setting. Geochemistry, 80: 125664.

Stephan A.L., 2014. Carbon sources and sinks within the Oman-UAE ophiolite: implications for natural atmospheric CO_2 sequestration rates. PhD thesis, Univ. Leicester (UK).

Sun S.S. and McDonough W.F., 1989. Chemical and isotopic systematics of oceanic basalts: Implications for mantle composition and processes. In: A.D. Saunders and M.J. Norry (Eds.). Magmatism in the Ocean Basins. Geol. Soc. London Spec. Publ., 42: 313-345.

Taylor S.R. and McLennan S.M., 1985. The Continental Crust: its composition and evolution: an examination of the geochemical record preserved in sedimentary rocks. Blackwell Sci. Publ., Oxford, 312 pp.

Tremblay A., Meshi A., Deschamps T., Goulet F. and Goulet N., 2015. The Vardar zone as a suture for the Mirdita ophiolites, Albania: Constraints from the structural analysis of the Korabi-Pelagonia zone. Tectonics, 34 (2): 352-375.

Vergély P. and Mercier J.-L., 2000. Données nouvelles sur les chevauchements d'âge post-Crétacé supérieur dans le massif du Paikon (zone de l'Axios-Vardar, Macédoine, Grèce): un nouveau modèle structural. C.R. Acad. Sci. Paris, Série IIA, 330: 555-561.

Wallace P.J., 2005. Volatiles in subduction zone magmas: concentrations and fluxes based on melt inclusion and volcanic gas data. J. Volcan. Geotherm. Res., 140: 217-240.

Walters J.B., Cruz-Uribe A.M. and Marschall H.R., 2019. Isotopic compositions of sulfides in exhumed high-pressure terranes: Implications for sulfur cycling in subduction zones. Geochem. Geophys. Geosyst., 20: 3347-3374.

Walters, J.B., Cruz-Uribe, A.M., and Marschall, H.R., 2020, Sulfur loss from subducted altered oceanic crust and implications for mantle oxidation. Geochem. Perspect. Lett., 13: 36-41.

Whattam S.A. and Stern R.J., 2011. The 'subduction initiation rule': a key for linking ophiolites, intra-oceanic forearcs, and subduction initiation. Contrib. Miner. Petrol. 162: 1031-1045.

Winchester J.A. and Floyd P.A., 1977. Geochemical discrimination of different magma series and their differentiation products using immobile elements. Chem. Geol., 20: 323-343.

Workman R.K. and Hart S.R., 2005. Major and trace element composition of the depleted MORB mantle (DMM). Earth Planet. Sci. Lett., 231: 53-72.

Zachariadis, 2007. Ophiolites of the eastern Vardar Zone, N. Greece. Unpubl. PhD thesis, J. Gutenberg Univ., Mainz, 131 pp.

Zellmer G.F., Edmonds M. and Straub S.M., 2015. Volatiles in subduction zone magmatism. In: G.F. Zellmer, M. Edmonds, S.M. Straub. The role of volatiles in the genesis, evolution and eruption of arc magmas. Geol. Soc. Spec. Publ. London, 410, p. 1-17.

Received, November 30, 2021
Accepted, April 10, 2022
First published online, April 2, 2022